

Stabilization of a Rigid Body Payload with Multiple Cooperative Quadrotors

Farhad A. Goodarzi

Post Doctoral Fellow
George Washington University
Washington, DC 20052
Email: fgoodarzi@gwu.edu

Taeyoung Lee

Associate Professor
George Washington University
Washington, DC 20052
Email: tylee@gwu.edu

This paper presents the full dynamics and control of arbitrary number of quadrotor unmanned aerial vehicles (UAV) transporting a rigid body. The rigid body is connected to the quadrotors via flexible cables where each flexible cable is modeled as a system of arbitrary number of serially-connected links. It is shown that a coordinate-free form of equations of motion can be derived for the complete model without any simplicity assumptions that commonly appear in other literature, according to Lagrangian mechanics on a manifold. A geometric nonlinear controller is presented to transport the rigid body to a fixed desired position while aligning all of the links along the vertical direction. A rigorous mathematical stability proof is given and the desirable features of the proposed controller are illustrated by numerical examples and experimental results.

Nomenclature

$i = 1, \dots, m$ m number of quadrotors
 n_i Number of links in the i -th cable
 $\vec{e}_1, \vec{e}_2, \vec{e}_3 \in \mathbb{R}^3$ Inertial frame
 $\vec{b}_1, \vec{b}_2, \vec{b}_3 \in \mathbb{R}^3$ Body-fixed frame of the payload
 $\vec{b}_{1_i}, \vec{b}_{2_i}, \vec{b}_{3_i} \in \mathbb{R}^3$ Body-fixed frame of the i -th quadrotor
 $m_i \in \mathbb{R}$ Mass of the i -th quadrotor
 $m_0 \in \mathbb{R}$ Mass of the payload
 $J_i \in \mathbb{R}^{3 \times 3}$ Inertia matrix of the i -th quadrotor
 $R_i \in \text{SO}(3)$ Attitude of the i -th quadrotor
 $\Omega_i \in \mathbb{R}^3$ Angular velocity of the i -th quadrotor
 $x_i \in \mathbb{R}^3$ Position of the i -th quadrotor
 $v_i \in \mathbb{R}^3$ Velocity of the i -th quadrotor
 $g \in \mathbb{R}$ Gravitational acceleration
 $\text{SO}(3)$ Special Orthogonal group
 $\text{SE}(3)$ Special Euclidean group

1 Introduction

Quadrotor UAVs are being considered for various missions such as Mars surface exploration, search and rescue, and particularly payload transportation. There are various applications for aerial load transportation such as usage in construction, military operations, emergency response, or delivering packages. Load transportation with UAVs can be performed using a cable or by grasping the payload [1, 2]. There are several limitations for grasping a payload with UAVs such as in situations where the landing area is inaccessible, or, it transporting a heavy/bulky object by multiple quadrotors.



Fig. 1. Two quadrotors stabilizing a payload cooperatively.

Load transportation with the cable-suspended load has been studied traditionally for a helicopter [3, 4] or for small

unmanned aerial vehicles such as quadrotor UAVs [5, 6, 7].

In most of the prior works, the dynamics of aerial transportation has been simplified due to the inherent dynamic complexities. For example, it is assumed that the dynamics of the payload is considered completely decoupled from quadrotors, and the effects of the payload and the cable are regarded as arbitrary external forces and moments exerted to the quadrotors [8, 9, 10], thereby making it challenging to suppress the swinging motion of the payload actively, particularly for agile aerial transportations.

Recently, the coupled dynamics of the payload or cable has been explicitly incorporated into control system design [11]. In particular, a complete model of a quadrotor transporting a payload modeled as a point mass, connected via a flexible cable is presented, where the cable is modeled as serially connected links to represent the deformation of the cable [12, 13]. In these studies the payload simplified and considered as a point mass without the attitude and the moment of inertia. In another study, multiple quadrotors transporting a rigid body payload has been studied [14], but it is assumed that the cables connecting the rigid body payload and quadrotors are always taut. These assumptions and simplifications in the dynamics of the system reduce the stability of the controlled system, particularly in rapid and aggressive load transportation where the motion of the cable and payload is excited nontrivially.

The other critical issue in designing controllers for quadrotors is that they are mostly based on local coordinates. Some aggressive maneuvers are demonstrated at [15] based on Euler angles. However they involve complicated expressions for trigonometric functions, and they exhibit singularities in representing quadrotor attitudes, thereby restricting their ability to achieve complex rotational maneuvers significantly. A quaternion-based feedback controller for attitude stabilization was shown in [16]. By considering the Coriolis and gyroscopic torques explicitly, this controller guarantees exponential stability. Quaternions do not have singularities but, as the three-sphere double-covers the special orthogonal group, one attitude may be represented by two antipodal points on the three-sphere. This ambiguity should be carefully resolved in quaternion-based attitude control systems, otherwise they may exhibit unwinding, where a rigid body unnecessarily rotates through a large angle even if the initial attitude error is small [17]. To avoid these, an additional mechanism to lift attitude onto the unit-quaternion space is introduced [18].

Recently, the dynamics of a quadrotor UAV is globally expressed on the special Euclidean group, $SE(3)$, and nonlinear control systems are developed to track outputs of several flight modes [19]. There are also several studies using the estimations for dynamical objects developed on the special Euclidean group [20, 21]. Several aggressive maneuvers of a quadrotor UAV are demonstrated based on a hybrid control architecture, and a nonlinear robust control system is also considered in [22, 23]. As they are directly developed on the special Euclidean/Orthogonal group, complexities, singularities, and ambiguities associated with minimal attitude representations or quaternions are completely avoided [24, 25].

The proposed control system is particularly useful for rapid and safe payload transportation in complex terrain, where the position of the payload should be controlled concurrently while suppressing the deformation of the cables.

Comparing with the prior work of the authors in [26, 27, 28] and other existing studies, this paper is the first study considering a complete model which includes a rigid body payload with attitude, arbitrary number of quadrotors, and flexible cables. A rigorous mathematical stability analysis is presented, and numerical and experimental validations in presence of uncertainties and disturbances are provided. More explicitly, we present the complete dynamic model of an arbitrary number of quadrotors transporting a rigid body where each quadrotor is connected to the rigid body via a flexible cable. Each flexible cable is modeled as an arbitrary number of serially connected links, and it is valid for various masses and lengths. A coordinate free form of equations of motion is derived according to Lagrange mechanics on a nonlinear manifold for the full dynamic model. These sets of equations of motion are presented in a complete and organized manner without any restrictive assumption or simplification.

Another contribution of this study is designing a control system to stabilize the rigid body at desired position. Geometric nonlinear controllers presented and generalized for the presented model. More explicitly, we show that the rigid body payload is asymptotically transported into a desired location, while aligning all of the links along the vertical direction corresponding to a hanging equilibrium. This paper presents a rigorous Lyapunov stability analysis for the proposed controller to establish stability properties without any timescale separation assumptions or singular perturbation, and a nonlinear integral control term is designed to guarantee robustness against unstructured uncertainties in both rotational and translational dynamics.

In short, new contributions and the unique features of the dynamics model and control system proposed in this paper compared with other studies are as follows: (i) it is developed for the full dynamic model of arbitrary number of multiple quadrotor UAVs on $SE(3)$ transporting a rigid body connected via flexible cables, including the coupling effects between the translational dynamics and the rotational dynamics on a nonlinear manifold, (ii) the control systems are developed directly on the nonlinear configuration manifold in a coordinate-free fashion. Thus, singularities of local parameterization are completely avoided to generate agile maneuvers in a uniform way, (iii) a rigorous Lyapunov analysis is presented to establish stability properties without any timescale separation assumption, and (iv) an integral control term is proposed to guarantee asymptotical convergence of tracking error variables in the presence of uncertainties, (v) the proposed algorithm is validated with experiments for payload transportation with multiple cooperative quadrotor UAVs. A rigorous and complete mathematical analysis for multiple quadrotor UAVs transporting a payload on $SE(3)$ with experimental validations for payload transportation maneuvers is unprecedented.

This paper is organized as follows. A dynamic model is

presented and the problem is formulated at Section II. Control systems are constructed at Sections III and IV, which are followed by numerical examples in Section V. Finally, experimental results are presented in Section VI.

2 Problem Formulation

Consider a rigid body with the mass $m_0 \in \mathbb{R}$ and the moment of inertia $J_0 \in \mathbb{R}^{3 \times 3}$, being transported with n arbitrary number of quadrotors as shown in Figure 2. The location of the mass center of the rigid body is denoted by $x_0 \in \mathbb{R}^3$, and its attitude is given by $R_0 \in \text{SO}(3)$, where the special orthogonal group is given by $\text{SO}(3) = \{R \in \mathbb{R}^{3 \times 3} \mid R^T R = I, \det(R) = 1\}$. We choose an inertial frame $\{\vec{e}_1, \vec{e}_2, \vec{e}_3\}$ and body fixed frame $\{\vec{b}_1, \vec{b}_2, \vec{b}_3\}$ attached to the payload. We also consider a body fixed frame attached to the i -th quadrotor $\{\vec{b}_{1i}, \vec{b}_{2i}, \vec{b}_{3i}\}$. In the inertial frame, the third axes \vec{e}_3 points downward along the gravity and the other axes are chosen to form an orthonormal frame.

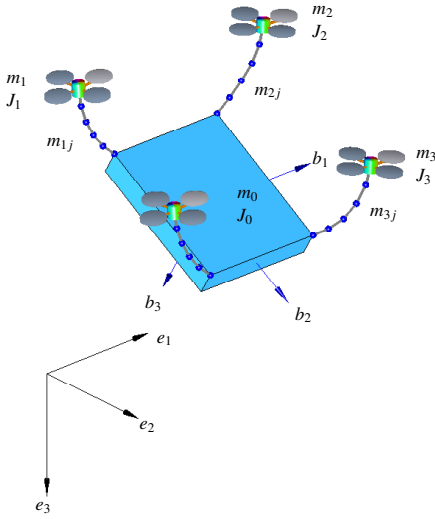


Fig. 2. Quadrotor UAVs with a rigid body payload. Cables are modeled as a serial connection of an arbitrary number of links (only 4 quadrotors with 5 links in each cable are illustrated).

The mass and the moment of inertia of the i -th quadrotor are denoted by $m_i \in \mathbb{R}$ and $J_i \in \mathbb{R}^{3 \times 3}$ respectively. The cable connecting each quadrotor to the rigid body is modeled as an arbitrary numbers of links for each quadrotor with varying masses and lengths. The direction of the j -th link of the i -th quadrotor, measured outward from the quadrotor toward the payload is defined by the unit vector $q_{ij} \in \mathbb{S}^2$, where $\mathbb{S}^2 = \{q \in \mathbb{R}^3 \mid \|q\| = 1\}$, where the mass and length of that link is denoted with m_{ij} and l_{ij} respectively. The number of links in the cable connected to the i -th quadrotor is defined as n_i . The configuration manifold for this system is given by $\text{SO}(3) \times \mathbb{R}^3 \times (\text{SO}(3))^n \times (\mathbb{S}^2)^{\sum_{i=1}^n n_i}$.

The i -th quadrotor can generate a thrust force of $-f_i R_i e_3 \in \mathbb{R}^3$ with respect to the inertial frame, where $f_i \in \mathbb{R}$ is the total thrust magnitude of the i -th quadrotor. It also generates a moment $M_i \in \mathbb{R}^3$ with respect to its body-fixed

frame. Also we define Δ_{x_i} and $\Delta_{R_i} \in \mathbb{R}^3$ as fixed disturbances applied to the i -th quadrotor's translational and rotational dynamics respectively. It is also assumed that an upper bound of the infinite norm of the uncertainty is known

$$\|\Delta_x\|_\infty \leq \delta, \quad (1)$$

for a positive constant δ . Throughout this paper, the two norm of a matrix A is denoted by $\|A\|$. The standard dot product is denoted by $x \cdot y = x^T y$ for any $x, y \in \mathbb{R}^3$.

2.1 Lagrangian

The kinematics equations for the links, payload, and quadrotors are given by

$$\dot{q}_{ij} = \omega_{ij} \times q_{ij} = \hat{\omega}_{ij} q_{ij}, \quad (2)$$

$$\dot{R}_0 = R_0 \hat{\Omega}_0, \quad (3)$$

$$\dot{R}_i = R_i \hat{\Omega}_i, \quad (4)$$

where $\omega_{ij} \in \mathbb{R}^3$ is the angular velocity of the j -th link in the i -th cable satisfying $q_{ij} \cdot \omega_{ij} = 0$. Also, $\Omega_0 \in \mathbb{R}^3$ is the angular velocity of the payload and $\Omega_i \in \mathbb{R}^3$ is the angular velocity of the i -th quadrotor, expressed with respect to the corresponding body fixed frame. The *hat map* $\hat{\cdot} : \mathbb{R}^3 \rightarrow \text{SO}(3)$ is defined by the condition that $\hat{x}y = x \times y$ for all $x, y \in \mathbb{R}^3$. More explicitly, for a vector $a = [a_1, a_2, a_3]^T \in \mathbb{R}^3$, the matrix \hat{a} is given by

$$\hat{a} = \begin{bmatrix} 0 & -a_3 & a_2 \\ a_3 & 0 & -a_1 \\ -a_2 & a_1 & 0 \end{bmatrix}. \quad (5)$$

This identifies the Lie algebra $\text{SO}(3)$ with \mathbb{R}^3 using the vector cross product in \mathbb{R}^3 . The inverse of the hat map is denoted by the *vee map*, $\vee : \text{SO}(3) \rightarrow \mathbb{R}^3$. The position of the i -th quadrotor is given by

$$x_i = x_0 + R_0 \rho_i - \sum_{a=1}^{n_i} l_{ia} q_{ia}, \quad (6)$$

where $\rho_i \in \mathbb{R}^3$ is the vector from the center of mass of the rigid body to the point that i -th cable is connected to the rigid body. Similarly the position of the j -th link in the cable connecting the i -th quadrotor to the rigid body is given by

$$x_{ij} = x_0 + R_0 \rho_i - \sum_{a=j+1}^{n_i} l_{ia} q_{ia}. \quad (7)$$

We derive equations of motion according to Lagrangian

mechanics. Total kinetic energy of the system is given by

$$T = \frac{1}{2}m_0\|\dot{x}_0\|^2 + \sum_{i=1}^n \sum_{j=1}^{n_i} \frac{1}{2}m_{ij}\|\dot{x}_{ij}\|^2 + \frac{1}{2} \sum_{i=1}^n m_i\|\dot{x}_i\|^2 + \frac{1}{2} \sum_{i=1}^n \Omega_i \cdot J_i \Omega_i + \frac{1}{2} \Omega_0 \cdot J_0 \Omega_0. \quad (8)$$

The gravitational potential energy is given by

$$V = -m_0 g e_3 \cdot x_0 - \sum_{i=1}^n m_i g e_3 \cdot x_i - \sum_{i=1}^n \sum_{j=1}^{n_i} m_{ij} g e_3 \cdot x_{ij}, \quad (9)$$

where it is assumed that the unit-vector e_3 points downward along the gravitational acceleration as shown at Figure 2. The corresponding Lagrangian of the system is $L = T - V$.

2.2 Euler-Lagrange equations

Coordinate-free form of Lagrangian mechanics on the two-sphere S^2 and the special orthogonal group $SO(3)$ for various multi-body systems has been studied in [29, 30]. The key idea is representing the infinitesimal variation of $R_i \in SO(3)$ in terms of the exponential map

$$\delta R_i = \left. \frac{d}{d\varepsilon} \right|_{\varepsilon=0} R_i \exp(\varepsilon \hat{\eta}_i) = R_i \hat{\eta}_i, \quad (10)$$

for $\eta_i \in \mathbb{R}^3$. The corresponding variation of the angular velocity is given by $\delta \Omega_i = \hat{\eta}_i + \Omega_i \times \eta_i$. Similarly, the infinitesimal variation of $q_{ij} \in S^2$ is given by

$$\delta q_{ij} = \xi_{ij} \times q_{ij}, \quad (11)$$

for $\xi_{ij} \in \mathbb{R}^3$ satisfying $\xi_{ij} \cdot q_{ij} = 0$. Using these, we obtain the following Euler-Lagrange equations.

Proposition 1. *The equations of motion for the proposed payload transportation system are as follows*

$$M_T \ddot{x}_0 - \sum_{i=1}^n \sum_{j=1}^{n_i} M_{0ij} l_{ij} \ddot{q}_{ij} - \sum_{i=1}^n M_{iT} R_0 \hat{\rho}_i \dot{\Omega}_0 = M_T g e_3 + \sum_{i=1}^n (-f_i R_i e_3 + \Delta_{x_i}) - \sum_{i=1}^n M_{iT} R_0 \hat{\Omega}_0^2 \rho_i, \quad (12)$$

$$\bar{J}_0 \dot{\Omega}_0 + \sum_{i=1}^n M_{iT} \hat{\rho}_i R_0^T \ddot{x}_0 - \sum_{i=1}^n \sum_{j=1}^{n_i} M_{0ij} l_{ij} \hat{\rho}_i R_0^T \ddot{q}_{ij} = \sum_{i=1}^n \hat{\rho}_i R_0^T (-f_i R_i e_3 + M_{iT} g e_3 + \Delta_{x_i}) - \hat{\Omega}_0 \bar{J}_0 \Omega_0, \quad (13)$$

$$\sum_{k=1}^{n_i} M_{0ij} l_{ik} \hat{q}_{ij}^2 \ddot{q}_{ik} - M_{0ij} \hat{q}_{ij}^2 \ddot{x}_0 + M_{0ij} \hat{q}_{ij}^2 R_0 \hat{\rho}_i \dot{\Omega}_0 = M_{0ij} \hat{q}_{ij}^2 R_0 \hat{\Omega}_0^2 \rho_i - \hat{q}_{ij}^2 (M_{0ij} g e_3 - f_i R_i e_3 + \Delta_{x_i}), \quad (14)$$

$$J_i \Omega_i + \Omega_i \times J_i \Omega_i = M_i + \Delta_{R_i}. \quad (15)$$

Here the total mass M_T of the system and the mass of the i -th quadrotor and its flexible cable M_{iT} are defined as

$$M_T = m_0 + \sum_{i=1}^n M_{iT}, \quad M_{iT} = \sum_{j=1}^{n_i} m_{ij} + m_i, \quad (16)$$

and the constants related to the mass of links are given as

$$M_{0ij} = m_i + \sum_{a=1}^{j-1} m_{ia}, \quad (17)$$

The equations of motion can be rearranged in a matrix form as follow

$$\mathbf{N} \dot{\mathbf{X}} = \mathbf{P} \quad (18)$$

where the state vector $X \in \mathbb{R}^{D_X}$ with $D_X = 6 + 3 \sum_{i=1}^n n_i$ is given by

$$\mathbf{X} = [\dot{x}_0, \Omega_0, \dot{q}_{1j}, \dot{q}_{2j}, \dots, \dot{q}_{nj}]^T, \quad (19)$$

and matrix $\mathbf{N} \in \mathbb{R}^{D_X \times D_X}$ is defined as

$$\mathbf{N} = \begin{bmatrix} M_T I_3 & \mathbf{N}_{x_0 \Omega_0} & \mathbf{N}_{x_0 1} & \mathbf{N}_{x_0 2} & \dots & \mathbf{N}_{x_0 n} \\ \mathbf{N}_{\Omega_0 x_0} & \bar{J}_0 & \mathbf{N}_{\Omega_0 1} & \mathbf{N}_{\Omega_0 2} & \dots & \mathbf{N}_{\Omega_0 n} \\ \mathbf{N}_{1 x_0} & \mathbf{N}_{1 \Omega_0} & \mathbf{N}_{q q 1} & 0 & \dots & 0 \\ \mathbf{N}_{2 x_0} & \mathbf{N}_{2 \Omega_0} & 0 & \mathbf{N}_{q q 2} & \dots & 0 \\ \vdots & \vdots & \vdots & \vdots & \vdots & \vdots \\ \mathbf{N}_{n x_0} & \mathbf{N}_{n \Omega_0} & 0 & 0 & \dots & \mathbf{N}_{q q n} \end{bmatrix}, \quad (20)$$

where the sub-matrices are defined as

$$\mathbf{N}_{x_0 \Omega_0} = - \sum_{i=1}^n M_{iT} R_0 \hat{\rho}_i; \quad \mathbf{N}_{\Omega_0 x_0} = \mathbf{M}_{x_0 \Omega_0}^T,$$

$$\mathbf{N}_{x_0 i} = -[M_{0i1} l_{i1} I_3, M_{0i2} l_{i2} I_3, \dots, M_{0in_i} l_{in_i} I_3],$$

$$\mathbf{N}_{\Omega_0 i} = -[M_{0i1} l_{i1} \hat{\rho}_i R_0^T, M_{0i2} l_{i2} \hat{\rho}_i R_0^T, \dots, M_{0in_i} l_{in_i} \hat{\rho}_i R_0^T],$$

$$\mathbf{N}_{i x_0} = -[M_{0i1} \hat{q}_{i1}^2, M_{0i2} \hat{q}_{i2}^2, \dots, M_{0in_i} \hat{q}_{in_i}^2]^T,$$

$$\mathbf{N}_{i \Omega_0} = [M_{0i1} \hat{q}_{i1}^2 R_0 \hat{\rho}_i, M_{0i2} \hat{q}_{i2}^2 R_0 \hat{\rho}_i, \dots, M_{0in_i} \hat{q}_{in_i}^2 R_0 \hat{\rho}_i]^T, \quad (21)$$

and the sub-matrix $\mathbf{N}_{qqi} \in \mathbb{R}^{3n_i \times 3n_i}$ is given by

$$\mathbf{N}_{qqi} = \begin{bmatrix} -M_{011} l_{i1} I_3 & M_{012} l_{i2} \hat{q}_{i2}^2 & \dots & M_{01n_i} l_{in_i} \hat{q}_{in_i}^2 \\ M_{021} l_{i1} \hat{q}_{i1}^2 & -M_{022} l_{i2} I_3 & \dots & M_{02n_i} l_{in_i} \hat{q}_{in_i}^2 \\ \vdots & \vdots & \ddots & \vdots \\ M_{0n_i 1} l_{i1} \hat{q}_{i1}^2 & M_{0n_i 2} l_{i2} \hat{q}_{i2}^2 & \dots & -M_{0n_i n_i} l_{in_i} I_3 \end{bmatrix}. \quad (22)$$

The $\mathbf{P} \in \mathbb{R}^{D_X}$ matrix is

$$\mathbf{P} = [P_{x_0}, P_{\Omega_0}, P_{1j}, P_{2j}, \dots, P_{nj}]^T, \quad (23)$$

and sub-matrices of \mathbf{P} matrix are also defined as

$$\begin{aligned} P_{x_0} &= M_T g e_3 + \sum_{i=1}^n (-f_i R_i e_3 + \Delta_{x_i}) - \sum_{i=1}^n M_{iT} R_0 \hat{\Omega}_0^2 \rho_i, \\ P_{\Omega_0} &= -\hat{\Omega}_0 \bar{J}_0 \Omega_0 + \sum_{i=1}^n \hat{\rho}_i R_0^T (M_{iT} g e_3 - f_i R_i e_3 + \Delta_{x_i}), \\ P_{ij} &= -\hat{q}_{ij}^2 (-f_i R_i e_3 + M_{0ij} g e_3 + \Delta_{x_i}) + M_{0ij} \hat{q}_{ij}^2 R_0 \hat{\Omega}_0^2 \rho_i \\ &\quad + M_{0ij} \|\dot{q}_{ij}\|^2 q_{ij}. \end{aligned}$$

Proof. See Appendix A.

These equations are derived directly on a nonlinear manifold without any simplification. The dynamics of the payload, flexible cables, and quadrotors are considered explicitly, and they avoid singularities and complexities associated to local coordinates.

3 CONTROL SYSTEM DESIGN FOR SIMPLIFIED DYNAMIC MODEL

3.1 Control Problem Formulation

Let $x_{0_d} \in \mathbb{R}^3$ be the desired position of the payload. The desired attitude of the payload is considered as $R_{0_d} = I_{3 \times 3}$, and the desired direction of links is aligned along the vertical direction. The corresponding location of the i -th quadrotor at this desired configuration is given by

$$x_{i_d} = x_{0_d} + \rho_i - \sum_{a=1}^{n_i} l_{ia} e_3. \quad (24)$$

We wish to design control forces f_i and control moments M_i of quadrotors such that this desired configuration becomes asymptotically stable.

3.2 Simplified Dynamic Model

Control forces for each quadrotor is given by $-f_i R_i e_3$ for the given equations of motion (12), (13), (14), (15). As such, the quadrotor dynamics is under-actuated. The total thrust magnitude of each quadrotor can be arbitrary chosen, but the direction of the thrust vector is always along the third body fixed axis, represented by $R_i e_3$. But, the rotational attitude dynamics of the quadrotors are fully actuated, and they are not affected by the translational dynamics of the quadrotors or the dynamics of links.

Based on these observations, in this section, we simplify the model by replacing the $-f_i R_i e_3$ term by a fictitious control input $u_i \in \mathbb{R}^3$, and design an expression for u_i to asymptotically stabilize the desired equilibrium. In other words, we assume that the attitude of the quadrotor can be instantaneously changed. Also Δ_{x_i} are ignored in the simplified dynamic model. The effects of the attitude dynamics are incorporated at the next section.

3.3 Linear Control System

The control system for the simplified dynamic model is developed based on the linearized equations of motion. At the desired equilibrium, the position and the attitude of the payload are given by x_{0_d} and $R_{0_d} = I_3$, respectively. Also, we have $q_{ij_d} = e_3$ and $R_{i_d} = I_3$. In this equilibrium configuration, the control input for the i -th quadrotor is

$$u_{i_d} = -f_{i_d} R_{i_d} e_3, \quad (25)$$

where the total thrust is $f_{i_d} = (M_{iT} + \frac{m_0}{n})g$.

The variation of x_0 is given by

$$\delta x_0 = x_0 - x_{0_d}, \quad (26)$$

and the variation of the attitude of the payload is defined as

$$\delta R_0 = R_{0_d} \hat{\eta}_0 = \hat{\eta}_0,$$

for $\eta_0 \in \mathbb{R}^3$. The variation of q_{ij} can be written as

$$\delta q_{ij} = \xi_{ij} \times e_3, \quad (27)$$

where $\xi_{ij} \in \mathbb{R}^3$ with $\xi_{ij} \cdot e_3 = 0$. The variation of ω_{ij} is given by $\delta \omega_{ij} \in \mathbb{R}^3$ with $\delta \omega_{ij} \cdot e_3 = 0$. Therefore, the third element of each of ξ_{ij} and $\delta \omega_{ij}$ for any equilibrium configuration is zero, and they are omitted in the following linearized equations. The state vector of the linearized equation is composed of $C^T \xi_{ij} \in \mathbb{R}^2$, where $C = [e_1, e_2] \in \mathbb{R}^{3 \times 2}$. The variation of the control input $\delta u_i \in \mathbb{R}^{3 \times 1}$, is given as $\delta u_i = u_i - u_{i_d}$.

Proposition 2. *The linearized equations of the simplified dynamic model are given by*

$$\mathbf{M} \ddot{\mathbf{x}} + \mathbf{G} \mathbf{x} = \mathbf{B} \delta u + \mathbf{g}(\mathbf{x}, \dot{\mathbf{x}}), \quad (28)$$

where $\mathbf{g}(\mathbf{x}, \dot{\mathbf{x}})$ corresponds to the higher order term and the state vector $\mathbf{x} \in \mathbb{R}^{D_x}$ with $D_x = 6 + 2 \sum_{i=1}^n n_i$ is given by

$$\mathbf{x} = [\delta x_0, \eta_0, C^T \xi_{1j}, C^T \xi_{2j}, \dots, C^T \xi_{nj}],$$

and $\delta u = [\delta u_1^T, \delta u_2^T, \dots, \delta u_n^T]^T \in \mathbb{R}^{3n \times 1}$. The matrix $\mathbf{M} \in \mathbb{R}^{D_x \times D_x}$ are defined as

$$\mathbf{M} = \begin{bmatrix} M_T I_3 & \mathbf{M}_{x_0 \Omega_0} & \mathbf{M}_{x_0 1} & \mathbf{M}_{x_0 2} & \cdots & \mathbf{M}_{x_0 n} \\ \mathbf{M}_{\Omega_0 x_0} & \bar{J}_0 & \mathbf{M}_{\Omega_0 1} & \mathbf{M}_{\Omega_0 2} & \cdots & \mathbf{M}_{\Omega_0 n} \\ \mathbf{M}_{1 x_0} & \mathbf{M}_{1 \Omega_0} & \mathbf{M}_{qq1} & 0 & \cdots & 0 \\ \mathbf{M}_{2 x_0} & \mathbf{M}_{2 \Omega_0} & 0 & \mathbf{M}_{qq2} & \cdots & 0 \\ \vdots & \vdots & \vdots & \vdots & \vdots & \vdots \\ \mathbf{M}_{n x_0} & \mathbf{M}_{n \Omega_0} & 0 & 0 & \cdots & \mathbf{M}_{qqn} \end{bmatrix},$$

where the sub-matrices are defined as

$$\begin{aligned} \mathbf{M}_{x_0\Omega_0} &= -\sum_{i=1}^n M_{iT} \hat{\rho}_i; \quad \mathbf{M}_{\Omega_0 x_0} = \mathbf{M}_{x_0\Omega_0}^T, \\ \mathbf{M}_{x_0i} &= [M_{0i1} l_{i1} \hat{e}_3 C, M_{0i2} l_{i2} \hat{e}_3 C, \dots, M_{0in_i} l_{in_i} \hat{e}_3 C], \\ \mathbf{M}_{\Omega_0 i} &= [M_{0i1} l_{i1} \hat{\rho}_i C, M_{0i2} l_{i2} \hat{\rho}_i C, \dots, M_{0in_i} l_{in_i} \hat{\rho}_i C], \\ \mathbf{M}_{ix_0} &= -[M_{0i1} C^T \hat{e}_3, M_{0i2} C^T \hat{e}_3, \dots, M_{0in_i} C^T \hat{e}_3], \quad (29) \\ \mathbf{M}_{i\Omega_0} &= [M_{0i1} C^T \hat{e}_3 \hat{\rho}_i, M_{0i2} C^T \hat{e}_3 \hat{\rho}_i, \dots, M_{0in_i} C^T \hat{e}_3 \hat{\rho}_i], \quad (30) \end{aligned}$$

and the sub-matrix $\mathbf{M}_{qqi} \in \mathbb{R}^{2n_i \times 2n_i}$ is given by

$$\mathbf{M}_{qqi} = \begin{bmatrix} M_{i11} l_{i1} I_2 & M_{i12} l_{i2} I_2 & \dots & M_{in_i} l_{in_i} I_2 \\ M_{i21} l_{i1} I_2 & M_{i22} l_{i2} I_2 & \dots & M_{i2n_i} l_{in_i} I_2 \\ \vdots & \vdots & \ddots & \vdots \\ M_{in_i 1} l_{i1} I_2 & M_{in_i 2} l_{i2} I_2 & \dots & M_{in_i n_i} l_{in_i} I_2 \end{bmatrix}. \quad (31)$$

The matrix $\mathbf{G} \in \mathbb{R}^{D_x \times D_x}$ is defined as

$$\mathbf{G} = \begin{bmatrix} 0 & 0 & 0 & 0 & 0 & 0 \\ 0 & \mathbf{G}_{\Omega_0 \Omega_0} & 0 & 0 & 0 & 0 \\ 0 & 0 & \mathbf{G}_1 & 0 & 0 & 0 \\ 0 & 0 & 0 & \mathbf{G}_2 & 0 & 0 \\ \vdots & \vdots & \vdots & \vdots & \vdots & \vdots \\ 0 & 0 & 0 & 0 & 0 & \mathbf{G}_n \end{bmatrix},$$

where $\mathbf{G}_{\Omega_0 \Omega_0} = \sum_{i=1}^n \frac{m_0}{n} g \hat{\rho}_i \hat{e}_3$ and the sub-matrices $\mathbf{G}_i \in \mathbb{R}^{2n_i \times 2n_i}$ are

$$\mathbf{G}_i = \text{diag} \left[\left(-M_{iT} - \frac{m_0}{n} + M_{0ij} \right) g e_3 I_2 \right].$$

The matrix $\mathbf{B} \in \mathbb{R}^{D_x \times 3n}$ is given by

$$\mathbf{B} = \begin{bmatrix} I_3 & I_3 & \dots & I_3 \\ \hat{\rho}_1 & \hat{\rho}_2 & \dots & \hat{\rho}_n \\ \mathbf{B}_B & 0 & 0 & 0 \\ 0 & \mathbf{B}_B & 0 & 0 \\ \vdots & \vdots & \vdots & \vdots \\ 0 & 0 & 0 & \mathbf{B}_B \end{bmatrix},$$

where $\mathbf{B}_B = -[C^T \hat{e}_3, C^T \hat{e}_3, \dots, C^T \hat{e}_3]^T$.

Proof. See Appendix B.

We present the following PD-type control system for the linearized dynamics

$$\delta u_i = -K_{x_i} \mathbf{x} - K_{\dot{x}_i} \dot{\mathbf{x}}, \quad (32)$$

for controller gains $K_{x_i}, K_{\dot{x}_i} \in \mathbb{R}^{3 \times D_x}$. Provided that (28) is controllable, we can choose the combined controller gains

$K_{\mathbf{x}} = [K_{x_1}^T, \dots, K_{x_n}^T]^T, K_{\dot{\mathbf{x}}} = [K_{\dot{x}_1}^T, \dots, K_{\dot{x}_n}^T]^T \in \mathbb{R}^{3n \times D_x}$ such that the equilibrium is asymptotically stable for the linearized equations [31]. Then, the equilibrium becomes asymptotically stable for the nonlinear Euler-Lagrange equation. The controlled linearized system can be written as

$$\dot{z}_1 = \mathbb{A} z_1 + \mathbb{B} (\mathbf{B} \mathbf{x} + \mathbf{g}(\mathbf{x}, \dot{\mathbf{x}})), \quad (33)$$

where $z_1 = [\mathbf{x}, \dot{\mathbf{x}}]^T \in \mathbb{R}^{2D_x}$ and

$$\mathbb{A} = \begin{bmatrix} 0 & I \\ -\mathbf{M}^{-1}(\mathbf{G} + \mathbf{B} K_{\mathbf{x}}) & -\mathbf{M}^{-1} \mathbf{B} K_{\dot{\mathbf{x}}} \end{bmatrix}, \mathbb{B} = \begin{bmatrix} 0 \\ \mathbf{M}^{-1} \end{bmatrix}. \quad (34)$$

We can also choose $K_{\mathbf{x}}$ and $K_{\dot{\mathbf{x}}}$ such that $\mathbb{A} \in \mathbb{R}^{2D_x \times 2D_x}$ is Hurwitz. Then for any positive definite matrix $Q \in \mathbb{R}^{2D_x \times 2D_x}$, there exist a positive definite and symmetric matrix $P \in \mathbb{R}^{2D_x \times 2D_x}$ such that $\mathbb{A}^T P + P \mathbb{A} = -Q$ according to [31, Thm 3.6].

4 CONTROL SYSTEM DESIGN FOR THE FULL DYNAMIC MODEL

The control system designed at the previous section is based on a simplifying assumption that each quadrotor can generate a thrust along any direction. In the full dynamic model, the direction of the thrust for each quadrotor is parallel to its third body-fixed axis always. In this section, the attitude of each quadrotor is controlled such that the third body-fixed axis becomes parallel to the direction of the ideal control force designed in the previous section. Also in the full dynamics model, we consider the Δ_{x_i} in the control design and introduce a new integral term to eliminate the disturbances and uncertainties. The central idea is that the attitude R_i of the quadrotor is controlled such that its total thrust direction $-R_i e_3$, corresponding to the third body-fixed axis, asymptotically follows the direction of the fictitious control input u_i . By choosing the total thrust magnitude properly, we can guarantee asymptotical stability for the full dynamic model.

Let $A_i \in \mathbb{R}^3$ be the ideal total thrust of the i -th quadrotor that asymptotically stabilize the desired equilibrium. Therefore, we have

$$A_i = u_{i_d} + \delta u_i = -K_{x_i} \mathbf{x} - K_{\dot{x}_i} \dot{\mathbf{x}} - K_z \text{sat}(e_{\mathbf{x}}) + u_{i_d}, \quad (35)$$

where $f_{i_d} \in \mathbb{R}$ and $u_{i_d} \in \mathbb{R}^3$ are the total thrust and control input of each quadrotor at its equilibrium respectively. where the following integral term $e_{\mathbf{x}} \in \mathbb{R}^{D_x}$ is added to eliminate the effect of disturbance Δ_{x_i} in the full dynamic model

$$e_{\mathbf{x}} = \int_0^t (P \mathbf{B})^T z_1(\tau) d\tau, \quad (36)$$

where $K_z = [k_z I_3, k_z I_3, k_{z_1} I_{3 \times 2}, \dots, k_{z_n} I_{3 \times 2}] \in \mathbb{R}^{3 \times D_x}$ is an integral gain. For a positive constant $\sigma \in \mathbb{R}$, a saturation function

$\text{sat}_\sigma : \mathbb{R} \rightarrow [-\sigma, \sigma]$ is introduced as

$$\text{sat}_\sigma(y) = \begin{cases} \sigma & \text{if } y > \sigma \\ y & \text{if } -\sigma \leq y \leq \sigma \\ -\sigma & \text{if } y < -\sigma \end{cases}.$$

If the input is a vector $y \in \mathbb{R}^n$, then the above saturation function is applied element by element to define a saturation function $\text{sat}_\sigma(y) : \mathbb{R}^n \rightarrow [-\sigma, \sigma]^n$ for a vector. From the desired direction of the third body-fixed axis of the i -th quadrotor, namely $b_{3_i} \in S^2$, is given by

$$b_{3_i} = -\frac{A_i}{\|A_i\|}. \quad (37)$$

This provides a two-dimensional constraint on the three dimensional desired attitude of each quadrotor, such that there remains one degree of freedom. To resolve it, the desired direction of the first body-fixed axis $b_{1_i}(t) \in S^2$ is introduced as a smooth function of time. Due to the fact that the first body-fixed axis is normal to the third body-fixed axis, it is impossible to follow an arbitrary command $b_{1_i}(t)$ exactly. Instead, its projection onto the plane normal to b_{3_i} is followed, and the desired direction of the second body-fixed axis is chosen to constitute an orthonormal frame [27]. More explicitly, the desired attitude of the i -th quadrotor is given by

$$R_{i_c} = \begin{bmatrix} -\frac{(\hat{b}_{3_i})^2 b_{1_i}}{\|(\hat{b}_{3_i})^2 b_{1_i}\|} & \frac{\hat{b}_{3_i} b_{1_i}}{\|\hat{b}_{3_i} b_{1_i}\|} & b_{3_i} \end{bmatrix}, \quad (38)$$

which is guaranteed to be an element of $\text{SO}(3)$. The desired angular velocity is obtained from the attitude kinematics equation, $\Omega_{i_c} = (R_{i_c}^T \dot{R}_{i_c})^\vee \in \mathbb{R}^3$.

Define the tracking error vectors for the attitude and the angular velocity of the i -th quadrotor as

$$e_{R_i} = \frac{1}{2} (R_{i_c}^T R_i - R_i^T R_{i_c})^\vee, \quad e_{\Omega_i} = \Omega_i - R_i^T R_{i_c} \Omega_{i_c}, \quad (39)$$

and a configuration error function on $\text{SO}(3)$ as follows

$$\Psi_i = \frac{1}{2} \text{tr}[I - R_{i_c}^T R_i]. \quad (40)$$

The thrust magnitude is chosen as the length of u_i , projected on to $-R_i e_3$, and the control moment is chosen as a tracking controller on $\text{SO}(3)$:

$$f_i = -A_i \cdot R_i e_3, \quad (41)$$

$$M_i = -k_R e_{R_i} - k_\Omega e_{\Omega_i} - k_I e_{I_i} + (R_i^T R_{c_i} \Omega_{c_i})^\wedge J_i R_i^T R_{c_i} \Omega_{c_i} + J_i R_i^T R_{c_i} \dot{\Omega}_{c_i}, \quad (42)$$

where k_R, k_Ω , and k_I are positive constants and the following integral term is introduced to eliminate the effect of fixed disturbance Δ_{R_i}

$$e_{I_i} = \int_0^t e_{\Omega_i}(\tau) + c_2 e_{R_i}(\tau) d\tau, \quad (43)$$

where c_2 is a positive constant. Stability of the corresponding controlled systems for the full dynamic model can be studied by showing the the error due to the discrepancy between the desired direction b_{3_i} and the actual direction $R_i e_3$.

Proposition 3. *Consider control inputs f_i, M_i defined in (41) and (42). There exist controller parameters and gains such that, (i) the zero equilibrium of tracking error is stable in the sense of Lyapunov; (ii) the tracking errors $e_{R_i}, e_{\Omega_i}, \mathbf{x}, \dot{\mathbf{x}}$ asymptotically converge to zero as $t \rightarrow \infty$; (iii) the integral terms e_{I_i} and e_x are uniformly bounded.*

Proof. See Appendix C.

By utilizing geometric control systems for quadrotor, we show that the hanging equilibrium of the links can be asymptotically stabilized while translating the payload to a desired position and attitude. The control systems proposed explicitly consider the coupling effects between the cable/load dynamics and the quadrotor dynamics. We presented a rigorous Lyapunov stability analysis to establish stability properties without any timescale separation assumptions or singular perturbation, and a new nonlinear integral control term is designed to guarantee robustness against unstructured uncertainties in both rotational and translational dynamics.

5 NUMERICAL EXAMPLE

We demonstrate the desirable properties of the proposed control system with numerical examples. Two cases are presented. At the first case, a payload is transported to a desired position from the ground. The second case considers stabilization of a payload with large initial attitude errors.

5.1 Stabilization of the Rigid Body

Consider four quadrotors ($n = 4$) connected via flexible cables to a rigid body payload. Initial conditions are chosen as

$$\begin{aligned} x_0(0) &= [1.0, 4.8, 0.0]^T \text{ m}, \quad v_0(0) = \mathbf{0}_{3 \times 1}, \\ q_{ij}(0) &= e_3, \quad \omega_{ij}(0) = \mathbf{0}_{3 \times 1}, \quad R_i(0) = I_{3 \times 3}, \quad \Omega_i(0) = \mathbf{0}_{3 \times 1} \\ R_0(0) &= I_{3 \times 3}, \quad \Omega_0 = \mathbf{0}_{3 \times 1}. \end{aligned}$$

The desired position of the payload is chosen as

$$x_{0_d}(t) = [0.44, 0.78, -0.5]^T \text{ m}. \quad (44)$$

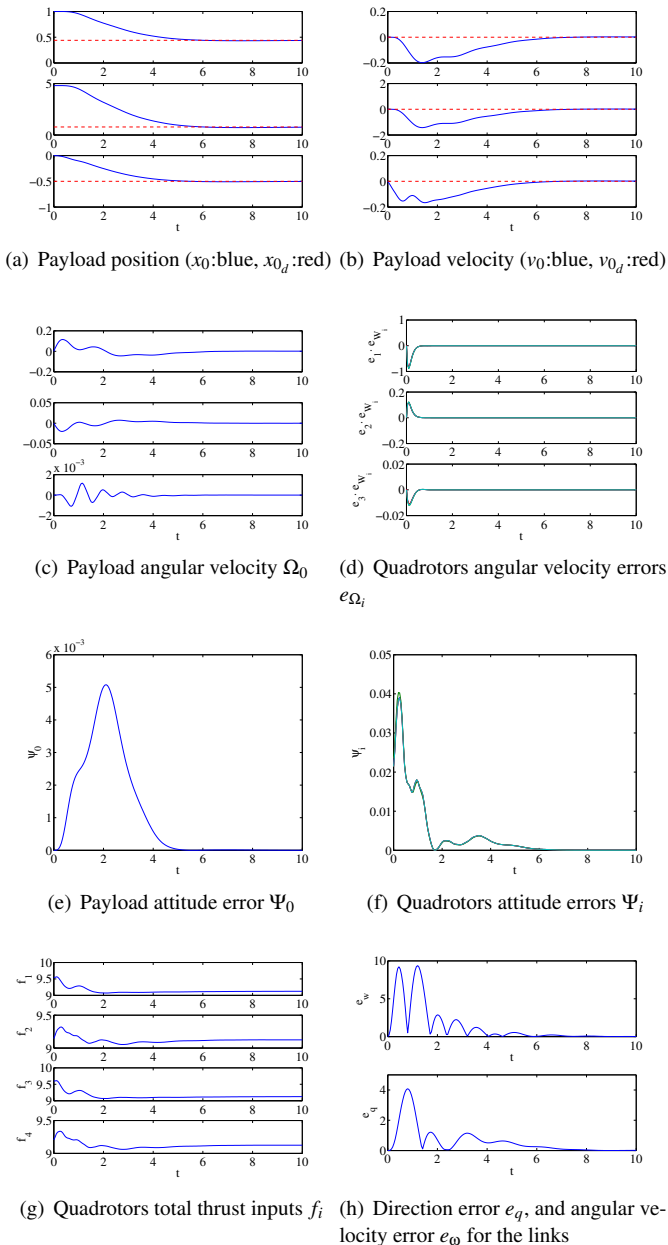


Fig. 3. Stabilization of a rigid-body connected to multiple quadrotors

The mass properties of quadrotors are chosen as

$$m_i = 0.755 \text{ kg},$$

$$J_i = \text{diag}[0.557, 0.557, 1.05] \times 10^{-2} \text{ kgm}^2. \quad (45)$$

The payload is a box with mass $m_0 = 0.5 \text{ kg}$, and its length, width, and height are 0.6, 0.8, and 0.2 m, respectively. Each cable connecting the rigid body to the i -th quadrotor is considered to be $n_i = 5$ rigid links. All the links have the same mass of $m_{ij} = 0.01 \text{ kg}$ and length of $l_{ij} = 0.15 \text{ m}$. Each cable

is attached to the following points of the payload

$$\rho_1 = [0.3, -0.4, -0.1]^T \text{ m}, \rho_2 = [0.3, 0.4, -0.1]^T \text{ m},$$

$$\rho_3 = [-0.3, -0.4, -0.1]^T \text{ m}, \rho_4 = [-0.3, 0.4, -0.1]^T \text{ m}.$$

Numerical simulation results are presented at Figure 3, which shows the position and velocity of the payload, and its tracking errors. We have also presented the link direction and link angular velocity errors defined as

$$e_q = \sum_{i=1}^m \sum_{j=1}^{n_i} \|q_{ij} - e_3\|, \quad (46)$$

$$e_\omega = \sum_{i=1}^m \sum_{j=1}^{n_i} \|\omega_{ij}\|. \quad (47)$$

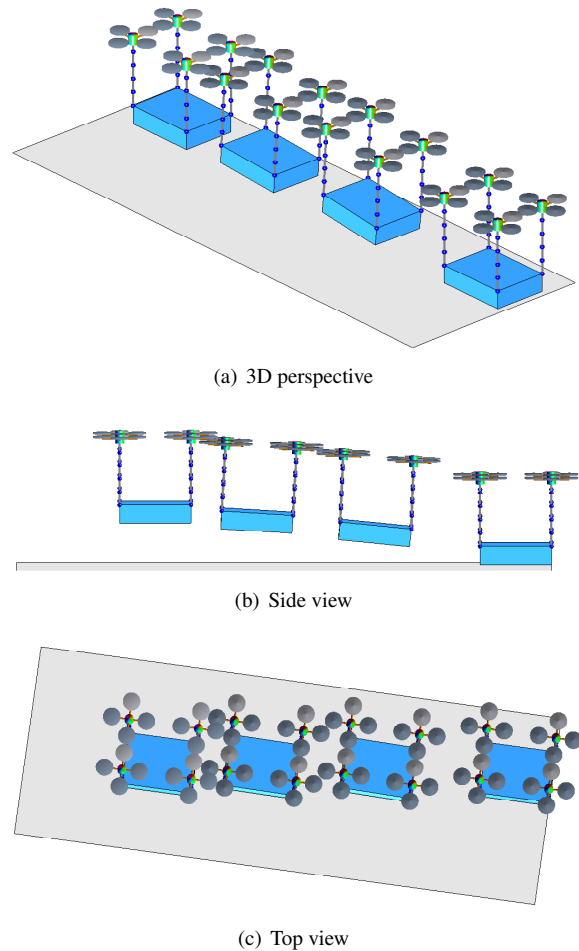


Fig. 4. Snapshots of controlled maneuver

5.2 Payload Stabilization with Large Initial Attitude Errors

In the second case, we consider large initial errors for the attitude of the payload and quadrotors. Initially, the rigid

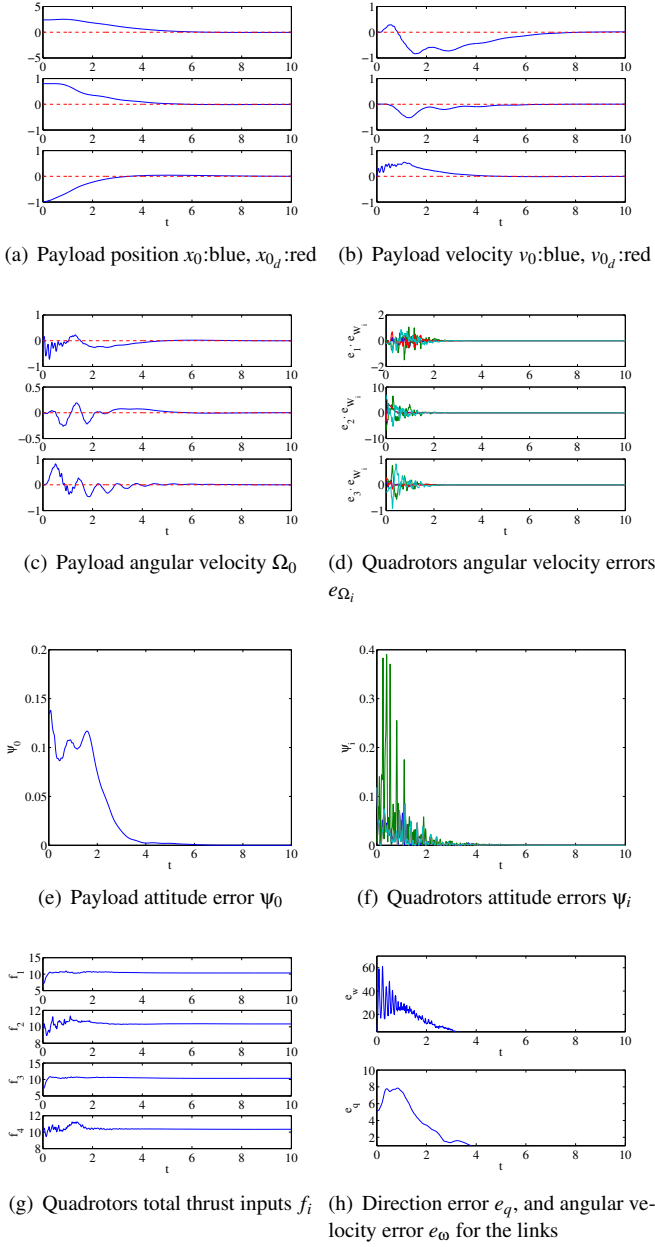


Fig. 5. Stabilization of a payload with multiple quadrotors connected with flexible cables.

body is tilted about its b_1 axis by 30 degrees, and the initial direction of the links are chosen such that two cables are curved along the horizontal direction. The initial conditions are given by

$$\begin{aligned} x_0(0) &= [2.4, 0.8, -1.0]^T, v_0(0) = 0_{3 \times 1}, \\ \omega_{ij}(0) &= 0_{3 \times 1}, \Omega_i(0) = 0_{3 \times 1} \\ R_0(0) &= R_x(30^\circ), \Omega_0 = 0_{3 \times 1}, \end{aligned}$$

where $R_x(30^\circ)$ denotes the rotation about the first axis by 30° . The initial attitude of quadrotors are chosen as

$$\begin{aligned} R_1(0) &= R_y(-35^\circ), R_2(0) = I_{3 \times 3}, \\ R_3(0) &= R_y(-35^\circ), R_4(0) = I_{3 \times 3}. \end{aligned}$$

The mass properties of quadrotors are chosen as pervious example. The payload is a box with mass $m_0 = 0.5$ kg, and its length, width, and height are 0.6, 0.8, and 0.2 m, respectively. Each cable connecting the rigid body to the i -th quadrotor is considered to be $n_i = 5$ rigid links. All the links have the same mass of $m_{ij} = 0.01$ kg and length of $l_{ij} = 0.15$ m. Each cable is attached to the following points of the payload

$$\begin{aligned} \rho_1 &= [0.3, -0.4, -0.1]^T \text{ m}, \rho_2 = [0.3, 0.4, -0.1]^T \text{ m}, \\ \rho_3 &= [-0.3, -0.4, -0.1]^T \text{ m}, \rho_4 = [-0.3, 0.4, -0.1]^T \text{ m}. \end{aligned}$$

The payload mass is $m = 1.0$ kg, and its length, width, and height are 1.0, 1.2, and 0.2 m, respectively.

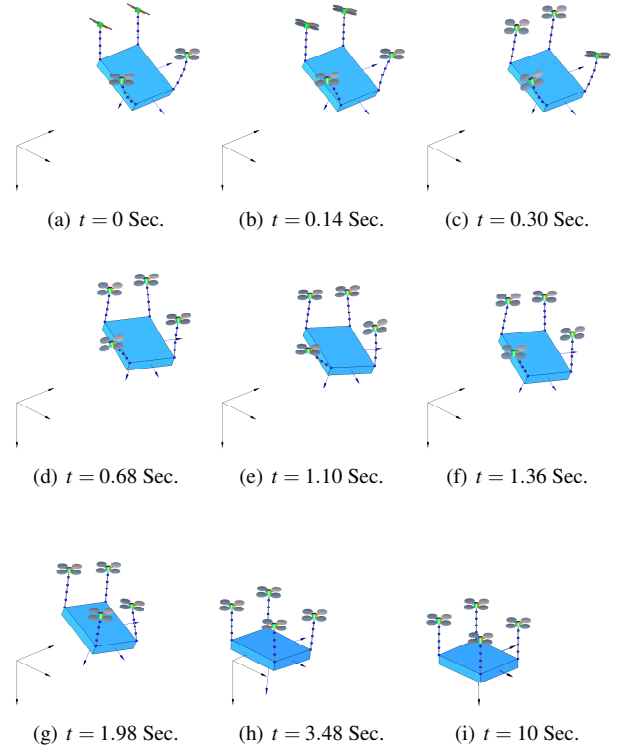


Fig. 6. Snapshots of the controlled maneuver. A short animation is also available at <https://www.youtube.com/watch?v=j14tSuHd8oA>

Figure 5 illustrates the tracking errors, and the total thrust of each quadrotor. Snapshots of the controlled maneuvers is also illustrated at Figure 6. It is shown that the proposed controller is able to stabilize the payload and cables at their desired configuration even from the large initial attitude errors.

6 EXPERIMENT

In this section, an experimental setup is described and the proposed geometric nonlinear controller is validated with experiments.

6.1 Hardware Description

The quadrotor UAV developed at the flight dynamics and control laboratory at the George Washington University is shown at Figure 7(a), and its parameters are the same as described as the previous section. The angular velocity is measured from inertial measurement unit (IMU) and the attitude is obtained from IMU data. Position of the UAV is measured from motion capture system (Vicon) and the velocity is estimated from the measurement. Ground computing system receives the Vicon data and send it to the UAV via XBee. The Gumstix is adopted as micro computing unit on the UAV. The flight control software has three main threads, namely Vicon thread, IMU thread, and control thread. The Vicon thread receives the Vicon measurement and estimates linear velocity of the quadrotor. In IMU thread, it receives the IMU measurement and estimates the attitude. The last thread handles the control outputs at each time step. Also, control outputs are calculated at 120Hz which is fast enough to run any kind of aggressive maneuvers. Information flow of the system is illustrated in Figure 9.

We developed an accurate CAD model as shown in Figure 8 to identify several parameters of the quadrotor, such as moment of inertia and center of mass. Furthermore, a precise rotor calibration is performed for each rotor, with a custom-made thrust stand as shown in Figure 7(b) to determine the relation between the command in the motor speed controller and the actual thrust. For various values of motor speed commands, the corresponding thrust is measured, and those data are fitted with a second order polynomial.

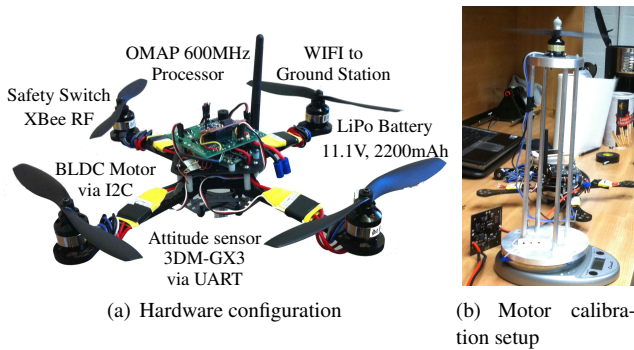


Fig. 7. Hardware development for each quadrotor UAV

6.2 Stabilizing a Rod with Two Quadrotors

As a special case of rigid body payload, we considered a rod as a payload for experiment as shown in the Figures 10. Two quadrotors are enough for this experiment to control the position of the payload.

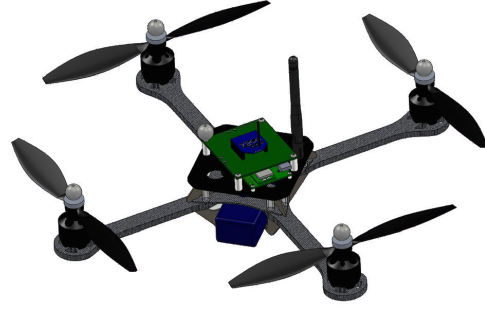


Fig. 8. CAD Model

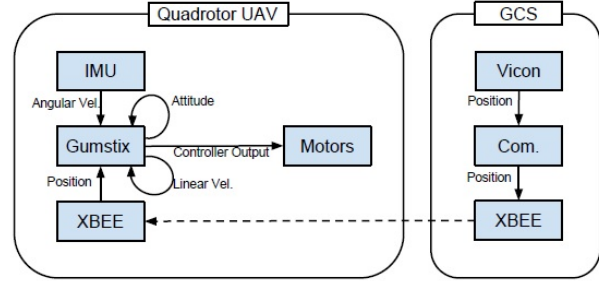


Fig. 9. Information flow of overall system

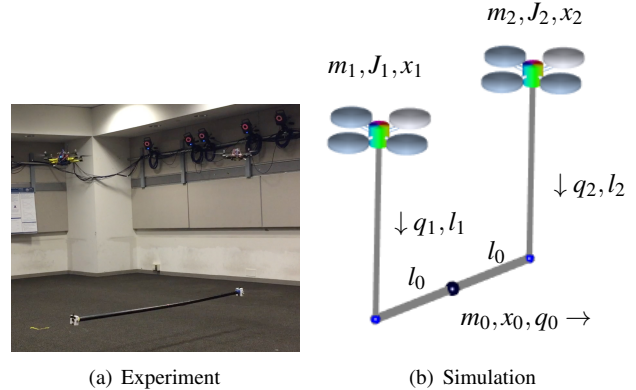


Fig. 10. Two quadrotors transporting a rod

We prepared a benchmark and a proposed controller case for this experiment. In both cases, two quadrotors are employed to hover at a fixed position initially while holding a rigid body rod which is at the equilibrium of the whole system. Then we utilized a wire to pull the payload and releasing it to simulate the disturbance. The performance of the proposed controller is then compared to the situation where there is no active controller specially works to stabilize the payload (benchmark). Both cables have length of $l_1, l_2 = 1.3 \text{ m}$ and rod has mass and length of $m_0 = 0.52 \text{ kg}$ and $2l_0 = 2.05 \text{ m}$ respectively. Each quadrotor has mass of $m_1 = m_2 = 0.755 \text{ kg}$ and the following moment of inertia

which is obtained from the CAD model

$$J_1, J_2 = \begin{bmatrix} 5.5711 & 0.0618 & -0.0251 \\ 0.06177 & 5.5757 & 0.0101 \\ -0.02502 & 0.01007 & 1.05053 \end{bmatrix} \times 10^{-2} \text{ kgm}^2.$$

The following relations and initial conditions is applied for both cases for this equilibrium condition

$$\begin{aligned} q_0(0) &= e_1, & q_1(0) &= q_2(0) = e_3, \\ x_1(0) &= x_0(0) - l_0 q_0(0) - l_1 q_1(0), \\ x_2(0) &= x_0(0) + l_0 q_0(0) - l_1 q_2(0), \\ R_1 &= R_2 = I_3, \\ \Omega_1 &= \Omega_2 = \Omega_0 = 0, \end{aligned}$$

6.2.1 Benchmark

We choose this case as a comparison benchmark and it's not the result of the proposed controller in this paper. In this case, two quadrotors are hovering above the payload while cables are aligned to the vertical direction and we apply a disturbance to the payload. Here, the cables and payload dynamics are not considered into the control system and geometric nonlinear controller is used for each quadrotor to maintain quadrotors hovering at the fixed position and considers the forces applied to the quadrotors from the payload as disturbance. The payload is pulled by 30° in the direction of y-axis of inertial frame and releases. The payload is oscillating below the quadrotors and forces applies to each quadrotor from the cables are just considered as disturbances to the quadrotors, so we experience large oscillations of the payload and cables.

Numerical results for this experiment are presented in Figures 11 which presents the first and second's link directions, position of the payload and positions of the quadrotors during this test.

6.2.2 Proposed Dynamical System and Controller

In this case, quadrotors are hovering at a fixed position using the geometric nonlinear controller while holding the payload. The payload is pulled with an external wire up to 30° angle same as the first case and then releases. Then, the proposed controller is switched in to stabilize the system. In this scenario, dynamic of the cables and payload are considered into the control system and quadrotors cooperatively work to stabilize the payload to the desired fixed position while aligning the cables in the vertical directions and the payload in the desired direction of first inertial axis, e_1 .

Figure 12 illustrates the position of the payload and quadrotors during this experiment where we applied the proposed controller. The vertical dotted line indicates the time when geometric nonlinear controller is switched with the proposed controller and stabilizes the system.

As shown in this figure, the proposed controller reduces and eliminates the oscillations of the cables and payload much effectively while considering the payload and cables

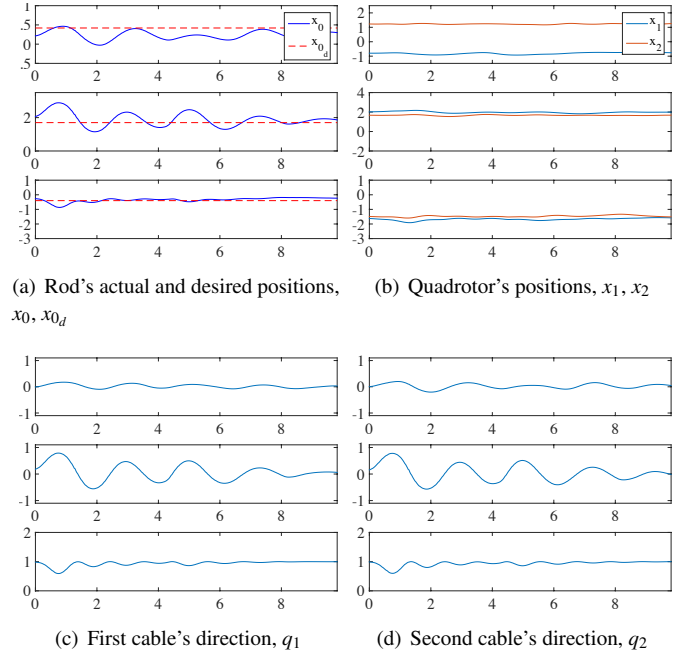


Fig. 11. Benchmark: quadrotor position control system [23]

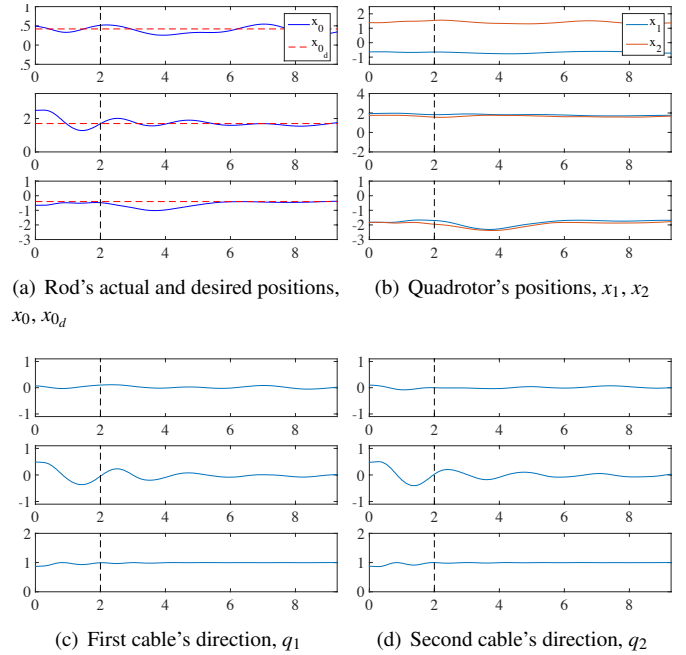


Fig. 12. Proposed Controller: two quadrotors with rigid body payload. (The vertical dotted line indicates the time when controller is switched in and stabilizes the system.)

dynamics. The desired cables directions are along the vertical direction $e_3 = [0, 0, 1]^T$ and the desired rod's directions is along the e_1 axis.

Snapshots of the controlled maneuvers is also illustrated at Figure 13.

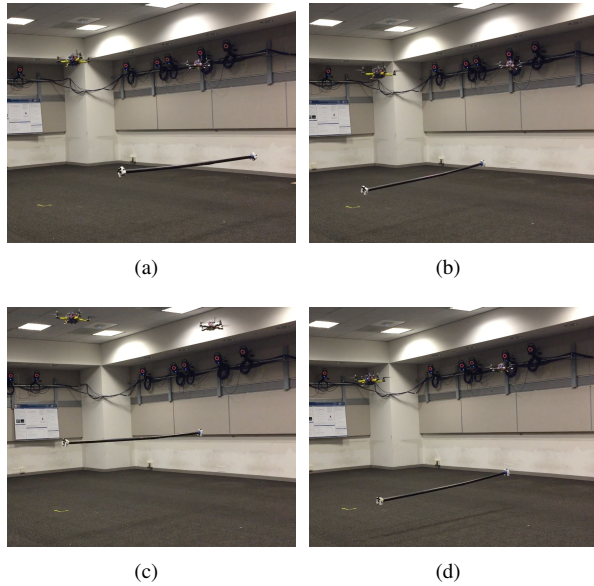


Fig. 13. Snapshots of controlled stabilization of a rod with two quadrotors. A short video of this comparison is available at <https://www.youtube.com/watch?v=u65Gqll2skY>

7 Conclusions

We utilized Euler-Lagrange equations to derive the complete model of multiple quadrotor UAVs transporting a rigid-body connected via flexible cables in 3D space. These derivations are developed in a remarkably compact form which allow us to choose an arbitrary number and any configuration of the links and an arbitrary number of quadrotors. We developed a geometric nonlinear controller to stabilize the links below the quadrotors and payload in the equilibrium position from an initial condition. We expanded these derivations in such a way that there is no need of using local angle coordinates which is an advantageous technique to signalize our derivations. A rigorous Lyapunov stability analysis is also presented to illustrate the stability properties without any time-scale separation. Numerical simulation and experimental results and for multiple cooperative quadrotors stabilizing a rigid-body performed and presented in this paper and shows the the accuracy and performance of the purposed model and control system.

Acknowledgements

This research has been supported in part by NSF under the grant CMMI-1243000 (transferred from 1029551), CMMI-1335008, and CNS-1337722.

References

[1] Mellinger, D., Shomin, M., Michael, N., and Kumar, V., 2013. “Cooperative grasping and transport using multiple quadrotors”. In *Distributed Autonomous Robotic Systems*, Vol. 83. Springer Berlin Heidelberg, pp. 545–558.

[2] Kim, S., Choi, S., and Kim, H. J., 2013. “Aerial manipulation using a quadrotor with a two dof robotic arm”. In *Intelligent Robots and Systems*, pp. 4990–4995.

[3] Cicolani, L., Kanning, G., and Synnestevedt, R., 1995. “Simulation of the dynamics of helicopter slung load systems”. *Journal of the American Helicopter Society*, **40**(4), pp. 44–61.

[4] Bernard, M., 2009. “Generic slung load transportation system using small size helicopters”. In *Proceedings of the International Conference on Robotics and Automation*, pp. 3258–3264.

[5] Palunko, I., Cruz, P., and Fierro, R., 2012. “Agile load transportation”. *IEEE Robotics and Automation Magazine*, **19**(3), pp. 69–79.

[6] Michael, N., Fink, J., and Kumar, V., 2011. “Cooperative manipulation and transportation with aerial robots”. *Autonomous Robots*, **30**, pp. 73–86.

[7] Maza, I., Kondak, K., Bernard, M., and Ollero, A., 2010. “Multi-UAV cooperation and control for load transportation and deployment”. *Journal of Intelligent and Robotic Systems*, **57**, pp. 417–449.

[8] Zamoski, D., Starr, G., Wood, J., and Lumia, R., 2008. “Rapid swing-free transport of nonlinear payloads using dynamic programming”. *Journal of Dynamic Systems, Measurement, and Control*, **130**(4), June, p. 041001.

[9] Schultz, J., and Murphey, T., 2012. “Trajectory generation for underactuated control of a suspended mass”. In *IEEE International Conference on Robotics and Automation*, pp. 123–129.

[10] Palunko, I., Fierro, R., and Cruz, P., 2012. “Trajectory generation for swing-free maneuvers of a quadrotor with suspended payload: A dynamic programming approach”. In *IEEE International Conference on Robotics and Automation*.

[11] Lee, T., Sreenath, K., and Kumar, V., 2013. “Geometric control of cooperating multiple quadrotor UAVs with a suspended load”. In *Proceedings of the IEEE Conference on Decision and Control*, Vol. 5510–5515.

[12] Goodarzi, F. A., Lee, D., and Lee, T., 2014. “Geometric stabilization of quadrotor UAV with a payload connected by flexible cable”. In *Proceedings of American Control Conference, Portland OR*, pp. 4925–4930.

[13] Goodarzi, F. A., Lee, D., and Lee, T., 2015. “Geometric control of a quadrotor uav transporting a payload connected via flexible cable”. *International Journal of Control, Automation and Systems*, **13**(6).

[14] Lee, T., 2014. “Dynamics and control of quadrotor uavs transporting a rigid body connected via flexible cables”. In *Proceedings of 53rd IEEE Conference on Decision and Control*, pp. 6155–6160.

[15] Mellinger, D., Michael, N., and Kumar, V., 2012. “Trajectory generation and control for precise aggressive maneuvers with quadrotors”. *International Journal Of Robotics Research*, **31**(5), pp. 664–674.

[16] Tayebi, A., and McGilvray, S., 2006. “Attitude stabilization of a VTOL quadrotor aircraft”. *IEEE Transactions on Control System Technology*, **14**(3), pp. 562–

- [17] Bhat, S., and Bernstein, D., 2000. “A topological obstruction to continuous global stabilization of rotational motion and the unwinding phenomenon”. *Systems and Control Letters*, **39**(1), pp. 66–73.
- [18] Mayhew, C., Sanfelice, R., and Teel, A., 2011. “Quaternion-based hybrid control for robust global attitude tracking”. *IEEE Transactions on Automatic Control*.
- [19] Goodarzi, F. A., Lee, D., and Lee, T., 2015. “Geometric adaptive tracking control of a quadrotor unmanned aerial vehicle on SE(3) for agile maneuvers”. *Journal of Dynamic Systems, Measurement, and Control*, **137**(9), September, pp. 091007–12.
- [20] Izadi, M., Bohn, J., Lee, D., Sanyal, A., Butcher, E., and Scheeres, D., 2013. “A nonlinear observer design for a rigid body in the proximity of a spherical asteroid”. In Proceedings of the ASME Dynamic Systems and Control Conference, Palo Alto, CA, USA.
- [21] Izadi, M., Sanyal, A., Barany, E., and Viswanathan, S., 2015. “Rigid body motion estimation based on the Lagrange–d’Alembert principle”. In Proceedings of the 54th IEEE Conference on Decision and Control.
- [22] Lee, T., Leok, M., and McClamroch, N., 2012. “Nonlinear robust tracking control of a quadrotor UAV on SE(3)”. In Proceeding of the American Control Conference, pp. 4649–4654.
- [23] Goodarzi, F., Lee, D., and Lee, T., 2013. “Geometric nonlinear PID control of a quadrotor UAV on SE(3)”. In Proceedings of the European Control Conference, pp. 3845–3850.
- [24] Chaturvedi, N., Sanyal, A., and McClamroch, N., 2011. “Rigid-body attitude control”. *IEEE Control Systems Magazine*, **31**(3), pp. 30–51.
- [25] Izadi, M., Sanyal, A., Beard, R., and Bai, H., 2015. “GPS-denied relative motion estimation for fixed-wing UAV using the variational pose estimator”. In Proceedings of the 54th IEEE Conference on Decision and Control.
- [26] Goodarzi, F. A., and Lee, T., 2015. “Dynamics and control of quadrotor UAVs transporting a rigid body connected via flexible cables”. In Proceedings of American Control Conference 2015, Chicago IL, pp. 4677–4682.
- [27] T. Lee, M. L., and McClamroch, N., 2013. “Nonlinear robust tracking control of a quadrotor UAV on SE(3)”. *Asian Journal of Control*, **15**(2), Mar., pp. 391–408.
- [28] Goodarzi, F. A., 2015. “Geometric nonlinear controls for multiple cooperative quadrotor UAVs transporting a rigid body”. PhD thesis, The George Washington University, August.
- [29] Lee, T., 2008. “Computational geometric mechanics and control of rigid bodies”. PhD thesis, University of Michigan.
- [30] Lee, T., Leok, M., and McClamroch, N. H., 2009. “Lagrangian mechanics and variational integrators on two-spheres”. *International Journal for Numerical Methods in Engineering*, **79**(9), pp. 1147–1174.
- [31] Khalil, H., 1996. *Nonlinear Systems*. Prentice Hall,

2nd Edition.

- [32] Fernando, T., Chandiramani, J., Lee, T., and Gutierrez, H., 2011. “Robust adaptive geometric tracking controls on SO(3) with an application to the attitude dynamics of a quadrotor uav”. In Proceedings of the IEEE Conference on Decision and Control, pp. 7380–7385.

A Proof for Proposition 1

A.1 Kinetic Energy

The kinetic energy of the whole system is composed of the kinetic energy of quadrotors, cables and the rigid body, as

$$T = \frac{1}{2}m_0\|\dot{x}_0\|^2 + \sum_{i=1}^n \sum_{j=1}^{n_i} \frac{1}{2}m_{ij}\|\dot{x}_{ij}\|^2 + \frac{1}{2} \sum_{i=1}^n m_i\|\dot{x}_i\|^2 + \frac{1}{2} \sum_{i=1}^n \Omega_i \cdot J_i \Omega_i + \frac{1}{2} \Omega_0 \cdot J_0 \Omega_0. \quad (48)$$

Substituting the derivatives of (6) and (7) into the above expression we have

$$T = \frac{1}{2}m_0\|\dot{x}_0\|^2 + \sum_{i=1}^n \sum_{j=1}^{n_i} \frac{1}{2}m_{ij}\|\dot{x}_0 + \dot{R}_0 \rho_i - \sum_{a=j+1}^{n_i} l_{ia} \dot{q}_{ia}\|^2 + \frac{1}{2} \sum_{i=1}^n m_i\|\dot{x}_0 + \dot{R}_0 \rho_i - \sum_{a=1}^{n_i} l_{ia} \dot{q}_{ia}\|^2 + \frac{1}{2} \sum_{i=1}^n \Omega_i \cdot J_i \Omega_i + \frac{1}{2} \Omega_0 \cdot J_0 \Omega_0. \quad (49)$$

We expand the above expression as follow

$$T = \frac{1}{2}(m_0\|\dot{x}_0\|^2 + \sum_{i=1}^n \sum_{j=1}^{n_i} m_{ij}\|\dot{x}_0\|^2 + \sum_{i=1}^n m_i\|\dot{x}_0\|^2) + \frac{1}{2} \sum_{i=1}^n (\sum_{j=1}^{n_i} m_{ij}\|\dot{R}_0 \rho_i\|^2 + m_i\|\dot{R}_0 \rho_i\|^2) + \sum_{i=1}^n (\sum_{j=1}^{n_i} m_{ij} \dot{x}_0 \cdot \dot{R}_0 \rho_i + m_i \dot{x}_0 \cdot \dot{R}_0 \rho_i) + \frac{1}{2} \sum_{i=1}^n (\sum_{j=1}^{n_i} m_{ij} \|\sum_{a=j+1}^{n_i} l_{ia} \dot{q}_{ia}\|^2 + m_i \|\sum_{a=1}^{n_i} l_{ia} \dot{q}_{ia}\|^2) - \sum_{i=1}^n (\sum_{j=1}^{n_i} m_{ij} \dot{x}_0 \cdot \sum_{a=j+1}^{n_i} l_{ia} \dot{q}_{ia} + \dot{x}_0 \cdot \sum_{a=1}^{n_i} l_{ia} \dot{q}_{ia}) - \sum_{i=1}^n (\sum_{j=1}^{n_i} m_{ij} \dot{R}_0 \rho_i \cdot \sum_{a=j+1}^{n_i} l_{ia} \dot{q}_{ia} + m_i \dot{R}_0 \rho_i \cdot \sum_{a=1}^{n_i} l_{ia} \dot{q}_{ia}) + \frac{1}{2} \sum_{i=1}^n \Omega_i \cdot J_i \Omega_i + \frac{1}{2} \Omega_0 \cdot J_0 \Omega_0, \quad (50)$$

and substituting (16), (17), it is rewritten as

$$\begin{aligned}
T = & \frac{1}{2} M_T \|\dot{x}_0\|^2 + \frac{1}{2} \sum_{i=1}^n M_{iT} \|\dot{R}_0 \rho_i\|^2 + \sum_{i=1}^n (M_{iT} \dot{x}_0 \cdot \dot{R}_0 \rho_i) \\
& + \sum_{i=1}^n \sum_{j,k=1}^{n_i} M_{0ij} l_{ik} \dot{q}_{ij} \cdot \dot{q}_{ik} - \sum_{i=1}^n (\dot{x}_0 \cdot \sum_{j=1}^{n_i} M_{0ij} l_{ij} \dot{q}_{ij}) \\
& - \sum_{i=1}^n (\dot{R}_0 \rho_i \cdot \sum_{j=1}^{n_i} M_{0ij} l_{ij} \dot{q}_{ij}) \\
& + \frac{1}{2} \sum_{i=1}^n \Omega_i \cdot J_i \Omega_i + \frac{1}{2} \Omega_0 \cdot J_0 \Omega_0. \tag{51}
\end{aligned}$$

A.2 Potential Energy

We can derive the potential energy expression by considering the gravitational forces on each part of system as given

$$V = -m_0 g e_3 \cdot x_0 - \sum_{i=1}^n m_i g e_3 \cdot x_i - \sum_{i=1}^n \sum_{j=1}^{n_i} m_{ij} g e_3 \cdot x_{ij}. \tag{52}$$

Using (6) and (7), we obtain

$$\begin{aligned}
V = & -m_0 g e_3 \cdot x_0 - \sum_{i=1}^n m_i g e_3 \cdot (x_0 + R_0 \rho_i - \sum_{a=1}^{n_i} l_{ia} q_{ia}) \\
& - \sum_{i=1}^n \sum_{j=1}^{n_i} m_{ij} g e_3 \cdot (x_0 + R_0 \rho_i - \sum_{a=j+1}^{n_i} l_{ia} q_{ia}), \tag{53}
\end{aligned}$$

and utilizing (17), we can simplify the potential energy as

$$V = -M_T g e_3 \cdot x_0 - \sum_{i=1}^n M_{iT} g e_3 \cdot R_0 \rho_i + \sum_{i=1}^n \sum_{j=1}^{n_i} M_{0ij} l_{ij} q_{ij} \cdot e_3. \tag{54}$$

A.3 Derivatives of Lagrangian

We develop the equation of motion for the Lagrangian $L = T - V$. The derivatives of the Lagrangian are given by

$$D_{\dot{x}_0} L = M_T \dot{x}_0 + \sum_{i=1}^n M_{iT} \dot{R}_0 \rho_i - \sum_{i=1}^n \sum_{j=1}^{n_i} M_{0ij} l_{ij} \dot{q}_{ij}, \tag{55}$$

$$D_{x_0} L = M_T g e_3, \tag{56}$$

$$D_{\dot{q}_{ij}} L = \sum_{i=1}^n \sum_{j=1}^{n_i} M_{0ij} l_{ik} \dot{q}_{ik} - \sum_{i=1}^n M_{0ij} l_{ij} (\dot{x}_0 + \dot{R}_0 \rho_i), \tag{57}$$

$$D_{q_{ij}} L = - \sum_{i=1}^n M_{0ij} l_{ij} e_3, \tag{58}$$

where $D_{\dot{x}_0}$ denote the derivative with respect to \dot{x}_0 , and other derivatives are defined similarly. We also have

$$\begin{aligned}
D_{\Omega_0} L = & J_0 \Omega_0 + \sum_{i=1}^n M_{iT} \hat{\rho}_i R_0^T \dot{x}_0, \\
& - \sum_{i=1}^n \sum_{j=1}^{n_i} M_{0ij} l_{ij} \hat{\rho}_i R_0^T \dot{q}_{ij} - \sum_{i=1}^n M_{iT} \hat{\rho}_i^2 \Omega_0, \tag{59}
\end{aligned}$$

which can be rewritten as

$$D_{\Omega_0} L = \bar{J}_0 \Omega_0 + \sum_{i=1}^n \hat{\rho}_i R_0^T (M_{iT} \dot{x}_0 - \sum_{j=1}^{n_i} M_{0ij} l_{ij} \dot{q}_{ij}), \tag{60}$$

where \bar{J}_0 is defined as

$$\bar{J}_0 = J_0 - \sum_{i=1}^n M_{iT} \hat{\rho}_i^2. \tag{61}$$

The derivative with respect to Ω_i is simply given by

$$D_{\Omega_i} L = \sum_{i=1}^n J_i \Omega_i. \tag{62}$$

The derivative of the Lagrangian with respect to R_0 along $\delta R_0 = R_0 \hat{\eta}_0$ is given by

$$\begin{aligned}
D_{R_0} L \cdot \delta R_0 = & \sum_{i=1}^n M_{iT} R_0 \hat{\eta}_0 \hat{\Omega}_0 \rho_i \cdot \dot{x}_0 \\
& - \sum_{i=1}^n R_0 \hat{\eta}_0 \hat{\Omega}_0 \rho_i \cdot \sum_{j=1}^{n_i} M_{0ij} l_{ij} \dot{q}_{ij} \\
& + \sum_{i=1}^n M_{iT} g e_3 \cdot R_0 \hat{\eta}_0 \rho_i, \tag{63}
\end{aligned}$$

which can be rewritten as

$$D_{R_0} L \cdot \delta R_0 = d_{R_0} \cdot \eta_0, \tag{64}$$

where

$$\begin{aligned}
d_{R_0} = & \sum_{i=1}^n (((\widehat{\hat{\Omega}_0} \rho_i R_0^T (M_{iT} \dot{x}_0) - \sum_{j=1}^{n_i} M_{0ij} l_{ij} \dot{q}_{ij}) \\
& + M_{iT} g \hat{\rho}_i R_0^T e_3)). \tag{65}
\end{aligned}$$

A.4 Lagrange-d'Alembert Principle

Consider $\mathcal{G} = \int_{t_0}^{t_f} L$ be the action integral. Using the equations derived in previous section, the infinitesimal vari-

ation of the action integral can be [9] written as

$$\begin{aligned} \delta\mathcal{E} = & \int_{t_0}^{t_f} D_{\dot{x}_0}L \cdot \delta\dot{x}_0 + D_{x_0} \cdot \delta x_0 \\ & + D_{\Omega_0}L(\dot{\eta}_0 + \Omega_0 \times \eta_0) + d_{R_0}L \cdot \eta_0 \\ & + \sum_{i=1}^n \sum_{j=1}^{n_i} D_{\dot{q}_{ij}}L(\dot{\xi}_{ij} \times q_{ij} + \xi_{ij} \times \dot{q}_{ij}) \\ & + \sum_{i=1}^n \sum_{j=1}^{n_i} D_{q_{ij}}L \cdot (\xi_{ij} \times q_{ij}) \\ & + \sum_{i=1}^n D_{\Omega_i}L \cdot (\dot{\eta}_i + \Omega_i \times \eta_i). \end{aligned} \quad (66)$$

The total thrust at the i -th quadrotor with respect to the inertial frame is denoted by $u_i = -f_i R_i e_3 \in \mathbb{R}^3$ and the total moment at the i -th quadrotor is defined as $M_i \in \mathbb{R}^3$. The corresponding virtual work due to the controls and disturbances is given by

$$\begin{aligned} \delta W = & \int_{t_0}^{t_f} \sum_{i=1}^n (u_i + \Delta_{x_i}) \cdot \{\delta x_0 + R_0 \hat{\eta}_0 \rho_i - \sum_{j=1}^{n_i} l_{ij} \dot{\xi}_{ij} \times q_{ij}\} \\ & + (M_i + \Delta_{R_i}) \cdot \eta_i dt. \end{aligned} \quad (67)$$

According to Lagrange-d'Alembert principle, we have $\delta\mathcal{E} = -\delta W$ for any variation of trajectories with fixed end points. By using integration by parts and rearranging, we obtain the following Euler-Lagrange equations

$$\frac{d}{dt} D_{\dot{x}_i}L - D_{x_0}L = \sum_{i=1}^n (u_i + \Delta_{x_i}), \quad (68)$$

$$\frac{d}{dt} D_{\Omega_0} + \Omega_0 \times D_{\Omega_0} - d_{R_0} = \sum_{i=1}^n \hat{\rho}_i R_0^T (u_i + \Delta_{x_i}), \quad (69)$$

$$\hat{q}_{ij} \frac{d}{dt} D_{\dot{q}_{ij}}L - \hat{q}_{ij} D_{q_i}L = -l_{ij} \hat{q}_{ij} (u_i + \Delta_{x_i}), \quad (70)$$

$$\frac{d}{dt} D_{\Omega_i}L + \Omega_i \times D_{\Omega_i}L = M_i + \Delta_{R_i}. \quad (71)$$

Substituting the derivatives of Lagrangians into the above expression and rearranging, the equations of motion are given by (12), (13), (14), (15).

B Proof for Proposition 2

The variations of x and q are given by (26) and (27). From the kinematics equation $\dot{q}_{ij} = \omega_{ij} \times q_{ij}$ and

$$\delta \dot{q}_{ij} = \dot{\xi}_{ij} \times e_3 = \delta \omega_{ij} \times e_3 + 0 \times (\xi_{ij} \times e_3) = \delta \omega_{ij} \times e_3.$$

Since both sides of the above equation is perpendicular to e_3 , this is equivalent to $e_3 \times (\dot{\xi}_{ij} \times e_3) = e_3 \times (\delta \omega_{ij} \times e_3)$, which yields

$$\dot{\xi}_{ij} - (e_3 \cdot \dot{\xi}_{ij})e_3 = \delta \omega_{ij} - (e_3 \cdot \delta \omega_{ij})e_3.$$

Since $\xi_{ij} \cdot e_3 = 0$, we have $\dot{\xi}_{ij} \cdot e_3 = 0$. As $e_3 \cdot \delta \omega_{ij} = 0$ from the constraint, we obtain the linearized equation for the kinematics equation of the link as

$$\dot{\xi}_{ij} = \delta \omega_{ij}. \quad (72)$$

The infinitesimal variation of $R_0 \in \text{SO}(3)$ in terms of the exponential map

$$\delta R_0 = \left. \frac{d}{d\varepsilon} \right|_{\varepsilon=0} R_0 \exp(\varepsilon \hat{\eta}_0) = R_0 \hat{\eta}_0, \quad (73)$$

for $\eta_0 \in \mathbb{R}^3$. Substituting these into (12), (13), and (14), and ignoring the higher order terms, we obtain the following sets of linearized equations of motion

$$\begin{aligned} M_T \delta \ddot{x}_0 - \sum_{i=1}^n M_{iT} \hat{\rho}_i \delta \dot{\Omega}_0 \\ + \sum_{i=1}^n \sum_{j=1}^{n_i} M_{0ij} l_{ij} \hat{e}_3 C(C^T \ddot{\xi}_{ij}) = \sum_{i=1}^n \delta u_i \end{aligned} \quad (74)$$

$$\begin{aligned} \sum_{i=1}^n M_{iT} \hat{\rho}_i \delta \ddot{x}_0 + \bar{J}_0 \delta \dot{\Omega}_0 + \sum_{i=1}^n \sum_{j=1}^{n_i} M_{0ij} l_{ij} \hat{\rho}_i \hat{e}_3 C(C^T \ddot{\xi}_{ij}) \\ + \sum_{i=1}^n \frac{m_0}{n} g \hat{\rho}_i \hat{e}_3 \eta_0 = \sum_{i=1}^n \hat{\rho}_i \delta u_i, \end{aligned} \quad (75)$$

$$\begin{aligned} -M_{0ij} C^T \hat{e}_3 \delta \ddot{x}_0 + M_{0ij} C^T \hat{e}_3 \hat{\rho}_i \delta \dot{\Omega}_0 + \sum_{k=1}^{n_i} M_{0ij} l_{ik} I_2 (C^T \ddot{\xi}_{ij}) \\ = -C^T \hat{e}_3 \delta u_i + (-M_{iT} - \frac{m_0}{n} + M_{0ij}) g e_3 I_2 (C^T \xi_{ij}), \end{aligned} \quad (76)$$

$$\hat{\eta}_i = \delta \Omega_i, \quad \hat{\eta}_0 = \delta \Omega_0, \quad J_i \delta \Omega_i = \delta M_i, \quad (77)$$

which can be written in a matrix form as presented in (28). We used $C^T \hat{e}_3^2 C = -I_2$ to simplify these derivations.

C Proof for Proposition 3

We first show stability of the rotational dynamics of each quadrotor, and later it is combined with the stability analysis for the remaining parts.

C.1 Attitude Error Dynamics

Here, the attitude error dynamics for e_{R_i} , e_{Ω_i} are derived and we find conditions on control parameters to guarantee the stability. The time-derivative of $J_i e_{\Omega_i}$ can be written as

$$J_i \dot{e}_{\Omega_i} = \{J_i e_{\Omega_i} + d_i\} \wedge e_{\Omega_i} - k_R e_{R_i} - k_{\Omega} e_{\Omega_i} - k_I e_{I_i} + \Delta_{R_i}, \quad (78)$$

where $d_i = (2J_i - \text{tr}[J_i]I)R_i^T R_{i,d} \Omega_{i,d} \in \mathbb{R}^3$ [23]. The important property is that the first term of the right hand side is normal to e_{Ω_i} , and it simplifies the subsequent Lyapunov analysis.

C.2 Stability for Attitude Dynamics

Define a configuration error function on $\text{SO}(3)$ as follows

$$\Psi_i = \frac{1}{2} \text{tr}[I - R_i^T R_i]. \quad (79)$$

We introduce the following Lyapunov function

$$\mathcal{V}_2 = \sum_{i=1}^n \mathcal{V}_{2i}, \quad (80)$$

where

$$\mathcal{V}_{2i} = \frac{1}{2} e_{\Omega_i} \cdot J_i \dot{e}_{\Omega_i} + k_R \Psi_i(R_i, R_{d_i}) + c_{2i} e_{R_i} \cdot e_{\Omega_i} \quad (81)$$

$$+ \frac{1}{2} k_I \|e_{I_i} - \frac{\Delta_{R_i}}{k_I}\|^2. \quad (82)$$

Consider a domain D_2 given by

$$D_2 = \{(R_i, \Omega_i) \in \text{SO}(3) \times \mathbb{R}^3 \mid \Psi_i(R_i, R_{d_i}) < \Psi_{2i} < 2\}. \quad (83)$$

In this domain we can show that \mathcal{V}_2 is bounded as follows [23]

$$\begin{aligned} z_{2i}^T M_{i21} z_{2i} + \frac{k_I}{2} \|e_{I_i} - \frac{\Delta_{R_i}}{k_I}\|^2 &\leq \mathcal{V}_{2i} \\ &\leq z_{2i}^T M_{i22} z_{2i} + \frac{k_I}{2} \|e_{I_i} - \frac{\Delta_{R_i}}{k_I}\|^2, \end{aligned} \quad (84)$$

where $z_{2i} = [\|e_{R_i}\|, \|e_{\Omega_i}\|]^T \in \mathbb{R}^2$ and matrices $M_{i21}, M_{i22} \in \mathbb{R}^{2 \times 2}$ are given by

$$\begin{aligned} M_{i21} &= \frac{1}{2} \begin{bmatrix} k_R & -c_{2i} \lambda_{M_i} \\ -c_{2i} \lambda_{M_i} & \lambda_{m_i} \end{bmatrix}, \\ M_{i22} &= \frac{1}{2} \begin{bmatrix} \frac{2k_R}{2-\Psi_{2i}} & c_{2i} \lambda_{M_i} \\ c_{2i} \lambda_{M_i} & \lambda_{M_i} \end{bmatrix}. \end{aligned}$$

The time derivative of \mathcal{V}_2 along the solution of the controlled system is given by

$$\begin{aligned} \dot{\mathcal{V}}_2 &= \sum_{i=1}^n -k_{\Omega} \|e_{\Omega_i}\|^2 - e_{\Omega_i} \cdot (k_I e_{I_i} - \Delta_{R_i}) \\ &\quad + c_{2i} \dot{e}_{R_i} \cdot J_i e_{\Omega_i} + c_{2i} e_{R_i} \cdot J_i \dot{e}_{\Omega_i} + (k_I e_{I_i} - \Delta_{R_i}) \dot{e}_{I_i}. \end{aligned}$$

We have $\dot{e}_{I_i} = c_2 e_{R_i} + e_{\Omega_i}$. Substituting (78), the above equation becomes

$$\begin{aligned} \dot{\mathcal{V}}_2 &= \sum_{i=1}^n -k_{\Omega} \|e_{\Omega_i}\|^2 + c_{2i} \dot{e}_{R_i} \cdot J_i e_{\Omega_i} - c_{2i} k_R \|e_{R_i}\|^2 \\ &\quad + c_{2i} e_{R_i} \cdot ((J_i e_{\Omega_i} + d_i)^\wedge e_{\Omega_i} - k_{\Omega} e_{\Omega_i}). \end{aligned}$$

We have $\|e_{R_i}\| \leq 1$, $\|\dot{e}_{R_i}\| \leq \|e_{\Omega_i}\|$ [32], and choose a constant B_{2i} such that $\|d_i\| \leq B_{2i}$. Then we obtain

$$\dot{\mathcal{V}}_2 \leq - \sum_{i=1}^n z_{2i}^T W_{2i} z_{2i}, \quad (85)$$

where the matrix $W_{2i} \in \mathbb{R}^{2 \times 2}$ is given by

$$W_{2i} = \begin{bmatrix} c_{2i} k_R & -\frac{c_{2i}}{2} (k_{\Omega} + B_{2i}) \\ -\frac{c_{2i}}{2} (k_{\Omega} + B_{2i}) & k_{\Omega} - 2c_{2i} \lambda_{M_i} \end{bmatrix}.$$

The matrix W_{2i} is a positive definite matrix if

$$c_{2i} < \min\left\{\frac{\sqrt{k_R \lambda_{m_i}}}{\lambda_{M_i}}, \frac{4k_{\Omega}}{8k_R \lambda_{M_i} + (k_{\Omega} + B_{2i})^2}\right\}. \quad (86)$$

This implies that

$$\dot{\mathcal{V}}_2 \leq - \sum_{i=1}^n \lambda_m(W_{2i}) \|z_{2i}\|^2, \quad (87)$$

which shows stability of the attitude dynamics of quadrotors.

C.3 Error Dynamics of the Payload and Links

We derive the tracking error dynamics and a Lyapunov function for the translational dynamics of a payload and the dynamics of links. Later it is combined with the stability analyses of the rotational dynamics. From (12), (28), (35), and (41), the equation of motion for the controlled dynamic model is given by

$$\mathbf{M}\ddot{\mathbf{x}} + \mathbf{G}\mathbf{x} = \mathbf{B}(u - u_d) + \mathbf{g}(\mathbf{x}, \dot{\mathbf{x}}) + \mathbf{B}\Delta_x, \quad (88)$$

where $\Delta_x \in \mathbb{R}^{3n \times 1}$ is

$$\Delta_x = [\Delta_{x_1} \ \Delta_{x_2} \ \cdots \ \Delta_{x_n}]^T, \quad (89)$$

and

$$u = \begin{bmatrix} u_1 \\ u_2 \\ \vdots \\ u_n \end{bmatrix}, \quad u_d = \begin{bmatrix} -(M_{1T} + \frac{m_0}{n}) g e_3 \\ -(M_{2T} + \frac{m_0}{n}) g e_3 \\ \vdots \\ -(M_{nT} + \frac{m_0}{n}) g e_3 \end{bmatrix}, \quad (90)$$

and $\mathbf{g}(\mathbf{x}, \dot{\mathbf{x}})$ corresponds to the higher order terms. As $u_i = -f_i R_i e_3$ for the full dynamic model, $\delta u = u - u_d$ is given by

$$\delta u = \begin{bmatrix} -f_1 R_1 e_3 + (M_{1T} + \frac{m_0}{n}) g e_3 \\ -f_2 R_2 e_3 + (M_{2T} + \frac{m_0}{n}) g e_3 \\ \vdots \\ -f_n R_n e_3 + (M_{nT} + \frac{m_0}{n}) g e_3 \end{bmatrix}. \quad (91)$$

The subsequent analyses are developed in the domain D_1

$$D_1 = \{(\mathbf{x}, \dot{\mathbf{x}}, R_i, e_{\Omega_i}) \in \mathbb{R}^{D_x} \times \mathbb{R}^{D_x} \times \text{SO}(3) \times \mathbb{R}^3 \mid \Psi_i < \psi_{1_i} < 1\}. \quad (92)$$

In the domain D_1 , we can show that

$$\frac{1}{2} \|e_{R_i}\|^2 \leq \Psi_i(R_i, R_{c_i}) \leq \frac{1}{2 - \psi_{1_i}} \|e_{R_i}\|^2. \quad (93)$$

Consider the quantity $e_3^T R_{c_i}^T R_i e_3$, which represents the cosine of the angle between $b_{3_i} = R_i e_3$ and $b_{3_{c_i}} = R_{c_i} e_3$. Since $1 - \Psi_i(R_i, R_{c_i})$ represents the cosine of the eigen-axis rotation angle between R_{c_i} and R_i , we have $e_3^T R_{c_i}^T R_i e_3 \geq 1 - \Psi_i(R_i, R_{c_i}) > 0$ in D_1 . Therefore, the quantity $\frac{1}{e_3^T R_{c_i}^T R_i e_3}$ is well-defined. We add and subtract $\frac{f_i}{e_3^T R_{c_i}^T R_i e_3} R_{c_i} e_3$ to the right hand side of (91) to obtain

$$\delta u = \begin{bmatrix} \frac{-f_1}{e_3^T R_{c_1}^T R_1 e_3} R_{c_1} e_3 - X_1 + (M_{1T} + \frac{m_0}{n}) g e_3 \\ \frac{-f_2}{e_3^T R_{c_2}^T R_2 e_3} R_{c_2} e_3 - X_2 + (M_{2T} + \frac{m_0}{n}) g e_3 \\ \vdots \\ \frac{-f_n}{e_3^T R_{c_n}^T R_n e_3} R_{c_n} e_3 - X_n + (M_{nT} + \frac{m_0}{n}) g e_3 \end{bmatrix}. \quad (94)$$

where $X_i \in \mathbb{R}^3$ is defined by

$$X_i = \frac{f_i}{e_3^T R_{c_i}^T R_i e_3} ((e_3^T R_{c_i}^T R_i e_3) R_i e_3 - R_{c_i} e_3). \quad (95)$$

Using

$$-\frac{f_i}{e_3^T R_{c_i}^T R_i e_3} R_{c_i} e_3 = -\frac{(\|A_i\| R_{c_i} e_3) \cdot R_i e_3}{e_3^T R_{c_i}^T R_i e_3} \cdot \frac{A_i}{\|A_i\|} = A_i, \quad (96)$$

the equation (94) becomes

$$\delta u = \begin{bmatrix} A_1 - X_1 + (M_{1T} + \frac{m_0}{n}) g e_3 \\ A_2 - X_2 + (M_{2T} + \frac{m_0}{n}) g e_3 \\ \vdots \\ A_n - X_n + (M_{nT} + \frac{m_0}{n}) g e_3 \end{bmatrix}. \quad (97)$$

Substituting (35) into the above equation, (88) becomes

$$\mathbf{M}\ddot{\mathbf{x}} + \mathbf{G}\mathbf{x} = \mathbf{B}(-K_x \mathbf{x} - K_x \dot{\mathbf{x}} - X - K_z \text{sat}(e_x) + \Delta_x) + \mathbf{g}(\mathbf{x}, \dot{\mathbf{x}}), \quad (98)$$

where $X = [X_1^T, X_2^T, \dots, X_n^T]^T \in \mathbb{R}^{3n}$. This can be rearranged as

$$\begin{aligned} \ddot{\mathbf{x}} = & -(\mathbf{M}^{-1} \mathbf{G} + \mathbf{M}^{-1} \mathbf{B} K_x) \mathbf{x} - (\mathbf{M}^{-1} \mathbf{B} K_x) \dot{\mathbf{x}} \\ & - \mathbf{M}^{-1} \mathbf{B} X - \mathbf{M}^{-1} \mathbf{B} K_z \text{sat}(e_x) + \mathbf{M}^{-1} \mathbf{g}(\mathbf{x}, \dot{\mathbf{x}}) + \mathbf{M}^{-1} \mathbf{B} \Delta_x. \end{aligned} \quad (99)$$

Using the definitions for \mathbb{A} , \mathbb{B} , and z_1 presented before, the above expression can be rearranged as

$$\dot{z}_1 = \mathbb{A} z_1 + \mathbb{B}(-\mathbf{B} X + \mathbf{g}(\mathbf{x}, \dot{\mathbf{x}}) - \mathbf{B} K_z \text{sat}(e_x) + \mathbf{B} \Delta_x). \quad (100)$$

C.4 Lyapunov Candidate for Simplified Dynamics

From the linearized control system developed at section 3, we use matrix P to introduce the following Lyapunov candidate for translational dynamics

$$\mathcal{V}_1 = z_1^T P z_1 + 2 \int_{p_{eq}}^{e_x} (\mathbf{B} K_z \text{sat}(\mu) - \mathbf{B} \Delta_x) \cdot d\mu. \quad (101)$$

The last integral term of the above equation is positive definite about the equilibrium point $e_x = p_{eq}$ where

$$p_{eq} = \left[\frac{\Delta_x}{k_z}, 0, 0, \dots \right], \quad (102)$$

if $\delta < k_z \sigma$, considering the fact that $\text{sat}_\sigma y = y$ if $y < \sigma$. The time derivative of the Lyapunov function using the Leibniz integral rule is given by

$$\dot{\mathcal{V}}_1 = \dot{z}_1^T P z_1 + z_1^T P \dot{z}_1 + 2 \dot{e}_x \cdot (\mathbf{B} K_z \text{sat}(e_x) - \mathbf{B} \Delta_x). \quad (103)$$

Since $\dot{e}_x^T = ((P\mathbb{B})^T z_1)^T = z_1^T P\mathbb{B}$ from (36), the above expression can be written as

$$\dot{\mathcal{V}}_1 = \dot{z}_1^T P z_1 + z_1^T P \dot{z}_1 + 2 z_1^T P\mathbb{B} (\mathbf{B} K_z \text{sat}(e_x) - \mathbf{B} \Delta_x). \quad (104)$$

Substituting (100) into (104), it reduces to

$$\dot{\mathcal{V}}_1 = z_1^T (\mathbb{A}^T P + P\mathbb{A}) z_1 + 2 z_1^T P\mathbb{B} (-\mathbf{B} X + \mathbf{g}(\mathbf{x}, \dot{\mathbf{x}})). \quad (105)$$

Let $c_3 = 2\|P\mathbb{B}\mathbb{B}\|_2 \in \mathbb{R}$ and using $\mathbb{A}^T P + P\mathbb{A} = -Q$, we have

$$\dot{\mathcal{V}}_1 \leq -z_1^T Q z_1 + c_3 \|z_1\| \|X\| + 2 z_1^T P\mathbb{B} \mathbf{g}(\mathbf{x}, \dot{\mathbf{x}}). \quad (106)$$

The second term on the right hand side of the above equation corresponds to the effects of the attitude tracking error on the translational dynamics. We find a bound of X_i , defined at (95), to show stability of the coupled translational dynamics

and rotational dynamics in the subsequent Lyapunov analysis. Since

$$f_i = \|A_i\| (e_3^T R_{c_i}^T R_i e_3), \quad (107)$$

we have

$$\|X_i\| \leq \|A_i\| \| (e_3^T R_{c_i}^T R_i e_3) R_i e_3 - R_{c_i} e_3 \|. \quad (108)$$

The last term $\| (e_3^T R_{c_i}^T R_i e_3) R_i e_3 - R_{c_i} e_3 \|$ represents the sine of the angle between $b_{3_i} = R_i e_3$ and $b_{3_{c_i}} = R_{c_i} e_3$, since $(b_{3_{c_i}} \cdot b_{3_i}) b_{3_i} - b_{3_{c_i}} = b_{3_i} \times (b_{3_i} \times b_{3_{c_i}})$. The magnitude of the attitude error vector, $\|e_{R_i}\|$ represents the sine of the eigen-axis rotation angle between R_{c_i} and R_i . Therefore, $\| (e_3^T R_{c_i}^T R_i e_3) R_i e_3 - R_{c_i} e_3 \| \leq \|e_{R_i}\|$ in D_1 . It follows that

$$\begin{aligned} \| (e_3^T R_{c_i}^T R_i e_3) R_i e_3 - R_{c_i} e_3 \| &\leq \|e_{R_i}\| = \sqrt{\Psi_i(2 - \Psi_i)} \\ &\leq \{ \sqrt{\Psi_i(2 - \Psi_i)} \triangleq \alpha_i \} < 1, \end{aligned} \quad (109)$$

therefore

$$\begin{aligned} \|X_i\| &\leq \|A_i\| \|e_{R_i}\| \\ &\leq \|A_i\| \alpha_i. \end{aligned} \quad (110)$$

We find an upper boundary for

$$A_i = -K_x \mathbf{x} - K_{\dot{\mathbf{x}}} \dot{\mathbf{x}} - K_z \text{sat}(e_{\mathbf{x}}) + u_{i_d}. \quad (111)$$

We define $K_{\max}, K_{z_m} \in \mathbb{R}$

$$\begin{aligned} K_{\max} &= \max\{\|K_x\|, \|K_{\dot{\mathbf{x}}}\|\}, \\ K_{z_m} &= \|K_z\|, \end{aligned}$$

by defining $\|u_{i_d}\| \leq B_{1_i}$, the upper bound of A_i is given by

$$\|A_i\| \leq K_{\max} (\|\mathbf{x}\| + \|\dot{\mathbf{x}}\|) + \sigma K_{z_m} + B_{1_i} \quad (112)$$

$$\leq 2K_{\max} \|z_1\| + (B_{1_i} + \sigma K_{z_m}), \quad (113)$$

Using the above steps we can show that

$$\begin{aligned} \|X\| &\leq \sum_{i=1}^n ((2K_{\max} \|z_1\| + (B_{1_i} + \sigma K_{z_m})) \|e_{R_i}\|) \\ &\leq (2K_{\max} \|z_1\| + (B_{1_i} + \sigma K_{z_m})) \alpha, \end{aligned} \quad (114)$$

where $\alpha = \sum_{i=1}^n \alpha_i$. Then, we can simplify (106) as

$$\begin{aligned} \dot{\mathcal{V}}_1 &\leq -(\lambda_{\min}(Q) - 2c_3 K_{\max} \alpha) \|z_1\|^2 \\ &\quad + \sum_{i=1}^n c_3 (B_{1_i} + \sigma K_{z_m}) \|z_1\| \|e_{R_i}\| + 2z_1^T P B g(\mathbf{x}, \dot{\mathbf{x}}). \end{aligned} \quad (115)$$

C.5 Lyapunov Candidate for the Complete System

Let $\mathcal{V} = \mathcal{V}_1 + \mathcal{V}_2$ be the Lyapunov function for the complete system. The time derivative of \mathcal{V} is given by

$$\dot{\mathcal{V}} = \dot{\mathcal{V}}_1 + \dot{\mathcal{V}}_2. \quad (116)$$

Substituting (115) and (87) into the above equation

$$\begin{aligned} \dot{\mathcal{V}} &\leq -(\lambda_{\min}(Q) - 2c_3 K_{\max} \alpha) \|z_1\|^2 + 2z_1^T P B g(\mathbf{x}, \dot{\mathbf{x}}) \\ &\quad + \sum_{i=1}^n c_3 (B_{1_i} + \sigma K_{z_m}) \|z_1\| \|e_{R_i}\| - \sum_{i=1}^n \lambda_m(W_{2_i}) \|z_{2_i}\|^2, \end{aligned} \quad (117)$$

and using $\|e_{R_i}\| \leq \|z_{2_i}\|$, it can be written as

$$\begin{aligned} \dot{\mathcal{V}} &\leq -(\lambda_{\min}(Q) - 2c_3 K_{\max} \alpha) \|z_1\|^2 + 2z_1^T P B g(\mathbf{x}, \dot{\mathbf{x}}) \\ &\quad + \sum_{i=1}^n c_3 (B_{1_i} + \sigma K_{z_m}) \|z_1\| \|z_{2_i}\| - \sum_{i=1}^n \lambda_m(W_{2_i}) \|z_{2_i}\|^2. \end{aligned} \quad (118)$$

The $2z_1^T P B g(\mathbf{x}, \dot{\mathbf{x}})$ term in the above equation is indefinite. But, the function $g(\mathbf{x}, \dot{\mathbf{x}})$ satisfies

$$\frac{\|g(\mathbf{x}, \dot{\mathbf{x}})\|}{\|z_1\|} \rightarrow 0 \quad \text{as} \quad \|z_1\| \rightarrow 0.$$

Then, for any $\gamma > 0$ there exists $r > 0$ such that

$$\|g(\mathbf{x}, \dot{\mathbf{x}})\| < \gamma \|z_1\| \quad \forall \|z_1\| < r.$$

Therefore

$$2z_1^T P B g(\mathbf{x}, \dot{\mathbf{x}}) \leq 2\gamma \|P\|_2 \|z_1\|^2. \quad (119)$$

Substituting the above inequality into (118)

$$\begin{aligned} \dot{\mathcal{V}} &\leq -(\lambda_{\min}(Q) - 2c_3 K_{\max} \alpha) \|z_1\|^2 + 2\gamma \|P\|_2 \|z_1\|^2 \\ &\quad + \sum_{i=1}^n c_3 (B_{1_i} + \sigma K_{z_m}) \|z_1\| \|z_{2_i}\| - \sum_{i=1}^n \lambda_m(W_{2_i}) \|z_{2_i}\|^2, \end{aligned} \quad (120)$$

and rearranging

$$\begin{aligned} \dot{\mathcal{V}} &\leq -\sum_{i=1}^n \left(\frac{\lambda_{\min}(Q) - 2c_3 K_{\max} \alpha}{n} \|z_1\|^2 \right. \\ &\quad \left. - c_3 (B_{1_i} + \sigma K_{z_m}) \|z_1\| \|z_{2_i}\| + \lambda_m(W_{2_i}) \|z_{2_i}\|^2 \right) \\ &\quad + 2\gamma \|P\|_2 \|z_1\|^2, \end{aligned} \quad (121)$$

we obtain

$$\dot{\mathcal{V}} \leq - \sum_{i=1}^n (\mathbf{z}_i^T W_i \mathbf{z}_i) + 2\gamma \|P\|_2 \|z_1\|^2, \quad (122)$$

where $\mathbf{z}_i = [\|z_1\|, \|z_{2i}\|]^T \in \mathbb{R}^2$ and

$$W_i = \begin{bmatrix} \frac{\lambda_{\min}(Q) - 2c_3(B_{1i} + \sigma K_{z_m})\alpha}{2} & -\frac{c_3 B_{1i}}{2} \\ -\frac{c_3(B_{1i} + \sigma K_{z_m})}{2} & \lambda_m(W_{2i}) \end{bmatrix}. \quad (123)$$

By using $\|z_1\| \leq \|\mathbf{z}_i\|$, we obtain

$$\dot{\mathcal{V}} \leq - \sum_{i=1}^n \left(\lambda_{\min}(W_i) - \frac{2\gamma \|P\|_2}{n} \right) \|\mathbf{z}_i\|^2. \quad (124)$$

Choosing $\gamma < n(\lambda_{\min}(W_i))/2\|P\|_2$, and

$$\lambda_m(W_{2i}) > \frac{n \left\| \frac{c_3(B_{1i} + \sigma K_{z_m})}{2} \right\|^2}{\lambda_{\min}(Q) - 2c_3 K_{\max} \alpha}, \quad (125)$$

ensures that $\dot{\mathcal{V}}$ is negative semi-definite. This implies that the zero equilibrium of tracking errors is stable in the sense of Lyapunov and \mathcal{V} is non-increasing. Therefore all of error variables z_1 , z_{2i} and integral control terms e_{I_i} , e_x are uniformly bounded. Also, from Lasalle-Yoshizawa theorem [31, Thm 3.4], we have $\mathbf{z}_i \rightarrow 0$ as $t \rightarrow \infty$.